Biogeochemistry
https://doi.org/10.1007/s10533-019-00587-0

Natural groundwater nutrient fluxes exceed anthropogenic inputs in an ecologically impacted estuary: lessons learned from Mobile Bay, Alabama

Daniel Montiel · Alexander F. Lamore · Jackson Stewart · W. Joe Lambert · Jacob Honeck · Yuehan Lu · Olivia Warren · Dini Adyasari · Nils Moosdorf · Natasha Dimova

Received: 27 February 2019 / Accepted: 22 August 2019

Abstract In this study we evaluated the magnitude and seasonal variations of natural and anthropogenic fluxes of inorganic (NO_3^-, NH_4^+, and PO_4^{3-}) and organic (DON and dissolved organic carbon) nutrients delivered by submarine groundwater discharge (SGD) and rivers to the fourth largest estuary in the USA, Mobile Bay in Alabama. To identify the sources of SGD-nutrient in the estuary and their subsurface biogeochemical transformation, we applied a multi-method approach that combines geochemical nutrient (N and P) mass-balances, stable isotopes (nitrate $\delta^{15}N_{NO_3}$ and $\delta^{18}O_{NO_3}$ and sediment organic matter $\delta^{13}C_{org}$ and $\delta^{15}N_{org}$) signatures, microbial sequencing analyses, dissolved organic matter source-composition, and shallow estuarine sediment lithological analyses. We found that during dry seasons SGD delivered nearly a quarter of the total nutrient inputs to Mobile Bay. These SGD fluxes were anoxic and N was delivered to the bay almost entirely as NH_4^+ and DON, which represented more than half of the total NH_4^+ and almost one fifth of the total DON inputs to the bay. We further observed that these significant

Responsible Editor: Sujay Kaushal

Electronic supplementary material The online version of this article (https://doi.org/10.1007/s10533-019-00587-0) contains supplementary material, which is available to authorized users.

D. Montiel (✉) · A. F. Lamore · J. Stewart · W. J. Lambert · J. Honeck · Y. Lu · O. Warren · N. Dimova
Department of Geological Sciences, University of Alabama, Tuscaloosa 35487, USA
e-mail: dmontielmartin@crimson.ua.edu

A. F. Lamore
e-mail: aflamore@crimson.ua.edu

J. Stewart
e-mail: jbstewart4@crimson.ua.edu

W. J. Lambert
e-mail: jlambert@ua.edu

J. Honeck
e-mail: jwhoneck@crimson.ua.edu

Y. Lu
e-mail: yuehan.lu@ua.edu

O. Warren
e-mail: omwarren@crimson.ua.edu

N. Dimova
e-mail: ntdimova@ua.edu

D. Montiel
Geosyntec Consultants, 50 South Belcher Road Suite 116, Clearwater 33765, USA

D. Adyasari · N. Moosdorf
Leibniz Centre for Tropical Marine Research (ZMT), Fahrenheitstraße 6, 28359 Bremen, Germany
e-mail: dini.adyasari@leibniz-zmt.de

N. Moosdorf
e-mail: nils.moosdorf@leibniz-zmt.de

Published online: 03 September 2019

SGD-derived N fluxes occurred exclusively to the east shore of Mobile Bay, historically impacted by hypoxia and large-scale fish kills known as "Jubilees". We demonstrate here that although the Mobile Bay coastal area is largely developed and anthropogenic influences are well documented, a shallow peat layer identified only on the east shore serves as the main source of the exceptionally high NH_4^+ and DON fluxes. We found that the high groundwater NO_3^- concentrations observed further inland from over-fertilization also identified by previous studies, decreased dramatically as groundwater percolated through the intertidal zone of the coastal aquifer. The microbial community identified in the coastal sediments suggests that denitrification and dissimilatory nitrate reduction to ammonium (DNRA) were the main processes responsible for this extensive removal and transformation of anthropogenic N, respectively. Furthermore, we found no significant anthropogenic inputs from manure or sewage waste to the bay. These findings show that natural sources of nutrients can outcompete anthropogenic inputs despite extensive development of the coastal area. We hypothesize that similar subsurface biogeochemical nutrient transformations can occur in other shallow estuaries of the northern Gulf of Mexico and worldwide.

Keywords Submarine groundwater discharge · Nutrient sources · Nutrient biogeochemical transformations · Estuary · *Jubilees* · Harmful algal blooms

Introduction

There is increasing evidence that estuaries worldwide are ecologically impacted by anthropogenic excess of nutrient inputs via submarine groundwater discharge (SGD; e.g. Johannes 1980; Moore 1999; Charette et al. 2001; Null et al. 2012; Xu et al. 2013). Due to longer residence time, dissolved constituents including nutrients, are usually enriched in groundwater, resulting in nutrient fluxes comparable to fluvial inputs (Charette et al. 2003; Santos et al. 2008). The excess of SGD-derived nutrient delivery in estuaries can cause eutrophication (Hwang et al. 2005), hypoxia (McCoy et al. 2011), seagrass beds degradation (Valiela et al. 1990), and harmful algal blooms (HABs; Garcés et al. 2011; Smith and Swarzenski 2012). Identifying the sources and fate of nutrients in the coastal aquifers as SGD occurs is critical for evaluating their ecological effects and improving management efforts in coastal areas (Knee and Paytan 2011).

In the intertidal zone, where the shallow SGD occurs, different forms of nitrogen (N) and phosphorous (P) nutrients undergo unique, yet intertwined pathways of biogeochemical transformations (Moore 1999; Seitzinger et al. 2002; Sadat-Noori et al. 2016). These changes are primarily controlled by site-specific coastal aquifer lithology, SGD residence time in the subsurface, redox conditions, and the rate and form of nutrient supply to the aquifer (Slomp and Van Cappellen 2004). The fast-growing population around many estuaries have raised concerns about the ecological implications of contaminants' inputs from agriculture, leaking septic systems, and inadequate manure managements, to mention a few (e.g. Valiela et al. 2000; Dowling et al. 2004; Kroeger et al. 2007; Knee and Paytan 2011; Null et al. 2012; Xu et al. 2013). To date, studies investigating the significance of naturally occurring sources of N and P in coastal systems are very limited (Slomp and Van Cappellen 2004; Knee and Paytan 2011). Nevertheless, in marsh and estuarine systems with inherently heterogeneous coastal aquifers and often organic-rich in content, there is evidence indicating that significant fluxes of N and P via SGD may have a natural origin (Krest et al. 2000; Kelly and Moran 2002; Moore et al. 2006; Null et al. 2011).

Estuaries are among the most diverse, productive, and economically important ecosystems. Located at the land–ocean interface, they are particularly sensitive to ecological disturbances due to rapid groundwater–surface water exchange and biogeochemical reactions (Seitzinger et al. 2002; Dulaiova et al. 2006; Burnett et al. 2007; Null et al. 2012; Xu et al. 2013; Makings et al. 2014). Most of the modern estuaries were formed after the last shoreline transgression when the sea level reached its present stage about 5000 years ago (Dyer 1973; Wolfe and Kjerfve 1986). The shallow coastal sediments of these estuaries reflect their dynamic geologic history and typically consist of alternating strata with significant variations in composition, organic matter content, and permeability (Krantz et al. 2004; Montiel et al. 2018). Because a large portion of SGD in estuaries occurs through the shallow intertidal sediments, the forms,

transformations, and concentrations of N- and P-nutrients in the discharging groundwater, and receiving surface waters, are modulated by this complex shallow lithological setting (Santos et al. 2009; Sadat-Noori et al. 2016; Cerdà-Domènech et al. 2017). The highly heterogeneous hydrogeology, combined with seasonal river flow fluctuations and daily tidal pumping generate particularly dynamic biogeochemical transformations of nutrients in the intertidal zone of estuaries (Krantz et al. 2004; Michael et al. 2016).

Mobile Bay, located in the Alabama Gulf Coast, is the fourth largest estuary in the USA (Fig. 1). Often during the summer (i.e. the dry season) Mobile Bay experiences large-scale fish and crustaceans kills locally known as "Jubilees" (Loesch 1960; Montiel et al. 2018). The economic impact of *Jubilees* is extensive, affecting recreational and commercial fisheries in Mobile Bay. In 1967 May (1973) estimated that during the *Jubilee* events that occurred between 1967 and 1971, 23,000 kg of fish, 18,000 kg of blue crabs, and 2,653,000 oysters died, accounting for a total value loss of $595,500 of that time. More recent studies indicate that HABs also occur systematically in Mobile Bay during the summer (Liefer et al. 2009; Macintyre et al. 2011; Su et al. 2014). These studies indicate that the *Jubilees* and HABs occur at specific locations of Mobile Bay, often in areas without direct surface water inputs (Loesch 1960; May 1973; Liefer et al. 2009). Although some understanding of the direct causes of *Jubilees* exists, the role of SGD in the recurrent development of hypoxia and the processes triggering and supporting the *Jubilees* has never been explored.

In this study, we investigated the sources, biogeochemical transformations, and main forms of N- and P-nutrients (NO_3^-, NH_4^+, DON, and PO_4^{3-}) delivered by SGD and local rivers to Mobile Bay (Alabama) to delineate the role of SGD for the development of hypoxia (i.e. *Jubilees*) and HAB events there. We used a multi-method approach based on nutrient mass-balances, stable isotopes analyses, description of the microbial community composition, organic matter characterizations, and lithological descriptions to identify and compare the magnitude of natural and anthropogenic sources of N and P delivered to the bay, specifically including areas impacted by hypoxia.

Research area

Mobile Bay has an area of 1.3×10^9 m^2, an average depth of 3.5 m, and a total volume of approximately 4.6×10^9 m^3. The main outlet of the estuary is Main Pass, connecting the bay with the Gulf of Mexico (GOM) in the south. Mobile Bay has a narrow (120 m) ship channel dredged to a depth of 15 m that extends from the City of Mobile to Main Pass (Greene et al. 2007; Du et al. 2018) (Fig. 1). As in all estuaries along the northern GOM, the tides in Mobile Bay are diurnal with an average tidal range of 0.4 m (Hummel 1996; Greene et al. 2007; Du et al. 2018). Although relatively shallow, Mobile Bay experiences strong vertical stratification during the summer (i.e. the dry season) under low river discharge and weak wind conditions (Schroeder and Wiseman 1986). Vertical temperature and salinity gradients generate a strong pycnocline that prevents physical mixing, contributing to extensive bottom waters hypoxia (May 1973; Turner et al. 1978).

The annual mean temperature in Mobile Bay is 21 °C, with a monthly maximum of 27 °C during the summer (June–August) and a minimum of 14 °C during the winter (December–February). Precipitation reaches maximum twice a year, once during the spring (February–March) and once during late summer (July–August), whereas the minimum usually occurs in June and October, with an annual mean of 1670 mm year^{-1} (Ward et al. 2005). Mobile Bay receives 95% of its surface water from the Mobile–Tensaw River System, the second largest river system in the GOM after the Mississippi–Atchafalaya River System (Dinnel et al. 1990). The Mobile–Tensaw River System has a drainage area of approximately 115,000 km^2 and an average daily discharge of 1500×10^5 m^3 day^{-1}, which flow is controlled mostly by precipitation throughout the year (Dinnel et al. 1990; Stumpf et al. 1993; Ward et al. 2005). Following the precipitation patterns, the river discharge peaks in March, while the minimum flow occurs during the late summer (July–September) when evapotranspiration is highest (Schroeder et al. 1990). Based on this annual trend, in this study we describe the summer months as the dry season and the spring as the wet season, with the exception of an extreme event in 2017 when the occurrence of tropical storm Cindy generated a rainfall exceeding that of March.

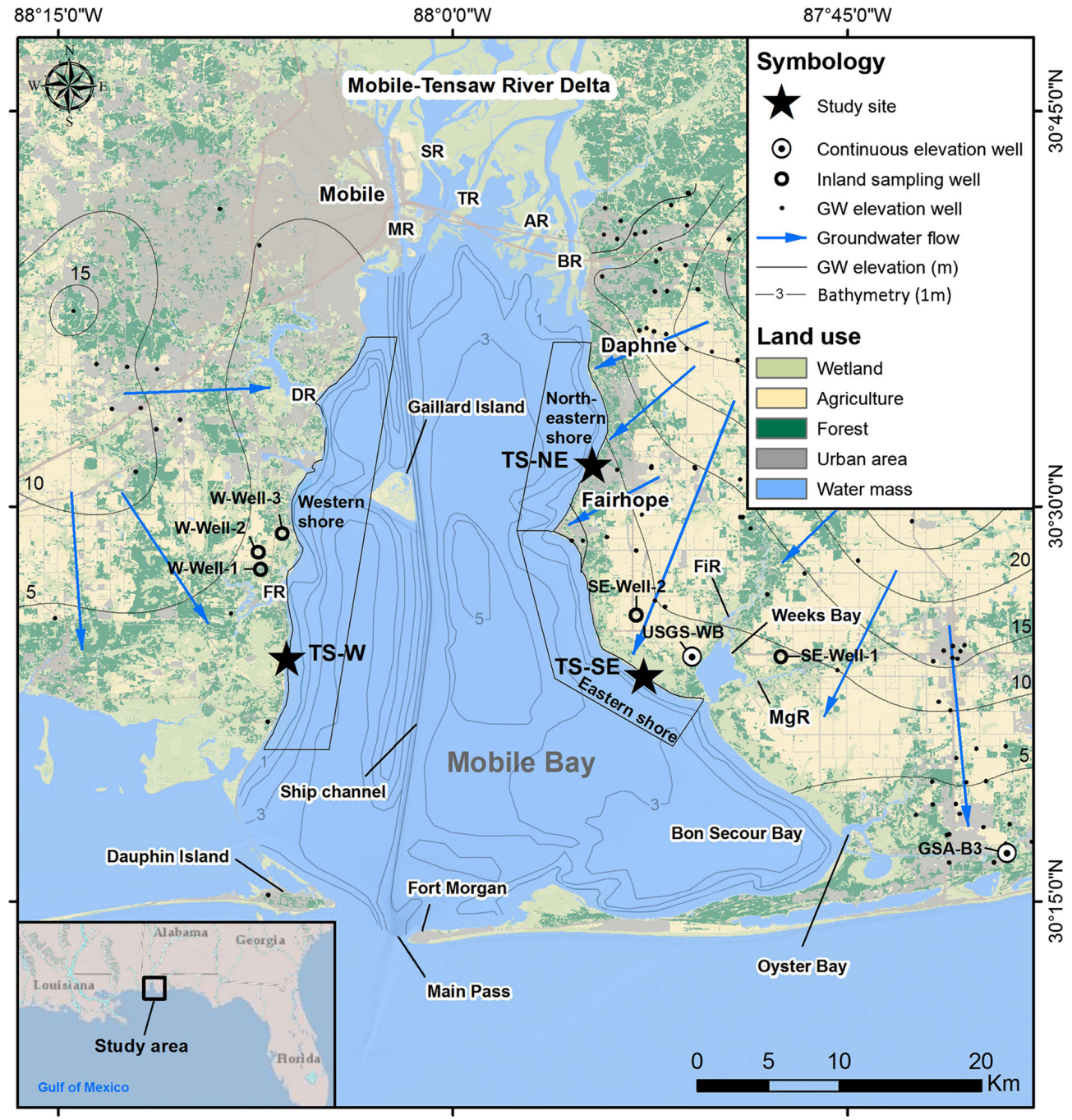

Fig. 1 Study area location, showing land uses (from Ellis et al. 2011), potentiometric surface of the Miocene–Pliocene Aquifer (Geological Survey of Alabama 2018), groundwater flow direction, monitoring wells for groundwater elevation, and sampled wells. The study area is divided in three sections: western shore, northeastern shore, and southeastern shore. At each section, the study sites where sediment core collection, intertidal piezometers installation (Pz-1–5), SGD assessments (Montiel et al. 2018), and SGD-derived nutrient fluxes evaluations were conducted, are represented with a star. Inland wells at both western and eastern shores are represented with an open circle. FR, DR, MR, SR, TR, AR, BR, FiR, and MgR represent the location of Fowl River, Dog River, Mobile River, Spanish River, Tensaw River, Apalachee River, Blakeley River, Fish River, and Magnolia River

About 80% of the Mobile–Tensaw River System watershed is covered by forests and wetlands, whereas agricultural lands comprise 18% and urban areas represent 2% (Ward et al. 2005). On the east shore of Mobile Bay, agriculture dominates the land use with 55% of the total area, whereas urban areas represent 5%, and scattered cattle farms represent 4%. The remaining 36% of this area is naturally preserved as forests (26%) and wetlands (10%) (Fig. 1). In contrast, on the west shore of the bay, natural areas of wetlands and forest dominate the land use with 39% and 22%, respectively, while the urbanized area of Mobile City occupies 20% and agriculture 19% (Ellis et al. 2011) (Fig. 1).

Two main aquifer units comprise the coastal hydrogeology of Mobile Bay: the Watercourse Aquifer and the Miocene–Pliocene Aquifer (Walter and Kidd 1979; Gillett et al. 2000; Montiel et al. 2018). Both units are hydraulically connected to Mobile Bay and are separated by a thin interbedded clay layer. The Watercourse Aquifer is a shallow (10–20 m) unconfined unit comprised of Pleistocene to Holocene sand deposits, present only in the southernmost sector of the western shore and Bon Secour Bay (Fig. 1). The Miocene–Pliocene Aquifer is an unconfined to semi-confined formation composed of sand deposits with a maximum thickness of 50–60 m (Reed 1971; Chandler et al. 1985; Gillett et al. 2000). The Miocene–Pliocene Aquifer water table elevation indicates that SGD could occur uniformly along the whole shoreline of Mobile Bay (Fig. 1) (Geological Survey of Alabama 2018). However, using radon (^{222}Rn) as a groundwater tracer, Montiel et al. (2018) found that SGD takes place preferentially along the east shore (80% of the total SGD) of Mobile Bay percolating through the shallow Miocene–Pliocene Aquifer (Fig. 1). These preferential pathways are the result of a combination of the regional topography and the lithological heterogeneity of the Miocene–Pliocene Aquifer coastal sediments. Additionally, using electrical resistivity tomography (ERT) and sediment cores Montiel et al. (2018) identified an organic-rich sediment layer with moderate hydraulic conductivity (8.2 m day^{-1}) underlain by the Miocene–Pliocene Aquifer that facilitates SGD on the east shore of Mobile Bay (Fig. 2b, c). Utilizing the same methods, they examined the western shore of Mobile Bay and found that a continuous silt formation of very low hydraulic conductivity (4.1 m day^{-1}), present uniformly along this section, restricts SGD in this area (Fig. 2a).

Methods

Sample collection

To identify the sources and evaluate the magnitude of nutrient inputs into Mobile Bay, we collected water samples representative of all nutrient end-members entering the system, including: (1) groundwater samples from the Miocene–Pliocene Aquifer in the inland and intertidal zones, (2) surface water from all tributaries of the Mobile–Tensaw River System entering the bay, and (3) surface water from Mobile Bay. All water samples were collected following the same protocol unless specified otherwise.

Surface water samples from Mobile Bay were collected during boat surveys conducted along the shoreline and across the bay during three wet seasons (March 2015, March 2016, and July 2017) and three dry seasons (July 2015, March 2017, and July 2018). During all surveys GPS positioning of the sampling locations was recorded in 30-s intervals (Lowrance HDS 5) with an accuracy of ± 1 m. The surface water was collected with a submersible pump from a depth of 0.3 m. Samples for nutrients (NO_3^-, NH_4^+, DON, and PO_4^{3-}), NO_3^- stable isotopes ($\delta^{15}N_{NO_3}$ and $\delta^{18}O_{NO_3}$), dissolved organic carbon (DOC), and dissolved organic matter (DOM) were filtered in the field with sterile 0.45 µm cellulose acetate filters and stored in acid-cleaned 50 mL polypropylene vials. Samples were kept in ice until arrival to the laboratory for a maximum of 6 h and frozen until analyses, except for DOM samples that were kept in the dark at 4 °C. River surface water samples were collected during all sampling campaigns from the tributaries of the Mobile–Tensaw River Delta, i.e. Mobile, Tensaw, Apalachee, and Blakeley Rivers at their point of discharge to the bay (Fig. 1).

Groundwater samples were collected from inland wells and shore-perpendicular transects of piezometers installed at study sites TS-W (western shore), TS-SE (southeastern shore), and TS-NE (northeastern shore) (Figs. 1, 2). The shore-perpendicular transects consisted of five piezometers (Pz-1–5) installed at different depths as illustrated in Fig. 2. Additionally, groundwater samples were also collected at study site TS-SE from a 2-m multi-level piezometer (SE-Pz-4.5). A detailed explanation of the piezometers installation can be found in Montiel et al. (2018).

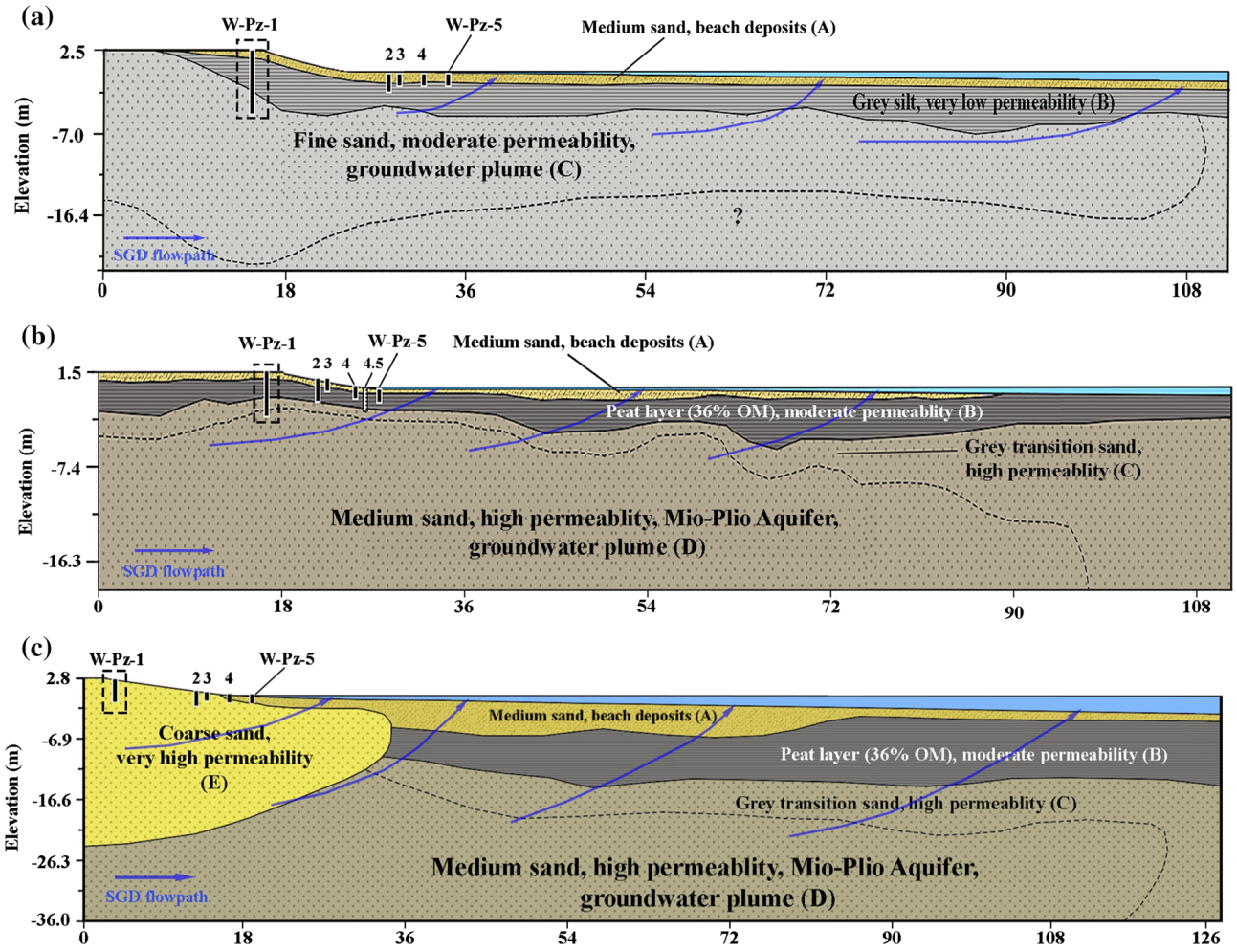

Fig. 2 Schematic geologic cross sections showing the lithologic characteristics of the shallow coastal sediments at study site TS-W on the western shore (**a**), TS-SE on the southeastern shore (**b**), and TS-NE on the northeastern shore (**c**) as presented in Montiel et al. (2018). The locations of all intertidal piezometers (Pz-1–5) and sediment cores (highlighted in dashed rectangles) are also shown on each panel. The dashed line represents the SGD plume extent on the western shore at TS-W (80 m), on the southeastern shore at TS-SE (70 m), and the northeastern shore at TS-NE (100 m)

Additionally, groundwater was collected from five preexisting deeper wells (10–12 m) on the western shore (W-Well-1–3) and the east shore (SE-Well-1 and -2) located 2–3 km inland from the shore (Fig. 1). Groundwater samples for microbial sequencing analyses were collected in duplicate 250 mL glass bottles and immediately filtered using 0.22 µm Merck isopore membrane filters, placed in a sterile 1.5 mL micro centrifuge tube, and stored frozen until analyses.

Shallow sediment cores (up to 4 m) were recovered using a Geoprobe coring system (Model 5410, Geoprobe Systems, Inc.) from the deepest piezometer (Pz-1) at each study site (cores TS-W, TS-SE, TS-NE in Fig. 2a–c). A detailed characterization of all sediment cores including density, porosity, grain size, hydraulic conductivity, and organic matter content can be found in Montiel et al. (2018).

Analytical methods

Dissolved oxygen (DO) in surface water and groundwater was measured using a Pro2030 (YSI, Inc.) handheld instrument with a galvanic sensor and a 1.25 mil polyethylene membrane with an accuracy of ± 0.2 mg L^{-1}. Before sampling, the DO sensor was calibrated following the YSI calibration procedure.

Nutrient (NO_3^-, NH_4^+, DON and PO_4^{3-}) analyses were performed at the Dauphin Island Sea Lab (DISL) using a Skalar San^{++} segmented flow autoanalyzer

with automatic in-line sample digestion (Skalar Analytical B.V.). The instrument analytical error was ± 5% for all nutrient measurements. Nitrite (NO_2^-) was also measured in all samples; however, NO_2^- concentrations represented less than 5% of the NO_3^- concentrations in approximately 90% of all samples. Therefore, NO_2^- was not reported here given that the instrument analytical error is ± 5%.

Nitrate stable isotopes $\delta^{15}N_{NO_3}$ and $\delta^{18}O_{NO_3}$ were analyzed at the UC Davis Stable Isotope Facility following the bacteria denitrification method (Sigman et al. 2001). Analyses were conducted using a GasBench$^+$ interfaced with a PreCon trace gas concentration system (Thermo Scientific, Inc.) interfaced to a Delta V isotope-ratio mass spectrometer (Thermo Scientific Inc.). Analytical precision for $\delta^{15}N_{NO_3}$ and $\delta^{18}O_{NO_3}$ are 0.4‰ and 0.5‰, respectively. Values of $\delta^{15}N_{NO_3}$ and $\delta^{18}O_{NO_3}$ were calculated relative to the atmospheric nitrogen standard (AIR) and the Vienna Standard Mean Ocean Water (VSMOW), respectively.

DOC concentrations in water were analyzed using a Shimadzu TOC-V total organic carbon analyzer (Shimadzu Scientific Instruments, Inc.) following the method described in Lu et al. (2015), with a standard deviation of duplicate measurements within 2%. To characterize DOM composition and identify sources (e.g., Hernes et al. 2009; Shang et al. 2018), DOM optical measurements were performed as described in Lu et al. (2015). Samples were analyzed using a 10-mm path length quartz cuvette on a UV-1800 Shimadzu UV–visible spectrophotometer (Shimadzu Scientific Instruments, Inc.) under the scanning wavelength from 190 to 670 nm at an interval of 1 nm. Three-dimensional fluorescence excitation–emission matrices were collected on a Horiba Jobin–Yvon Fluoromax-3 spectrofluorometer at the excitation wavelengths from 240 to 500 nm at 5 nm intervals and emission wavelengths from 280 to 538 nm at 3 nm intervals. Fluorescence components were identified via the parallel factor analysis (PARAFAC) in the DOMFluor toolbox (Stedmon and Bro 2008).

Molecular sequencing analyses of microbial communities were performed as described in Adyasari et al. (2019). Microbial community compositions were examined utilizing the 16S rRNA sequencing method on an Illumina Miseq. The DADA2 package was used to process the primer-clipped sequences (Callahan et al. 2016). Taxonomic classifications were determined with version 132 of the SILVA reference database. Primer-clipped sequence data from this study are available at the European Nucleotide Archive (ENA) with the Project Accession Number PRJEB33004, using the data brokerage service of the German Federation for Biological Data (Diepenbroek et al. 2014).

The organic matter of the organic-rich sediment layer (B) in core TS-SE (Fig. 2b) was analyzed at the Alabama Stable Isotope Laboratory (ASIL) for $\delta^{13}C_{org}$ and $\delta^{15}N_{org}$ stable isotope abundance, weight percent carbon (C-weight percent) and nitrogen (N-weight percent). Sediment samples were oven-dried at 50 °C for 16 h and homogenized with a mortar and pestle before analyses. The organic matter $\delta^{13}C$ and $\delta^{15}N$ were analyzed using an IRMS system consisting of an Elemental Combustion System (ECS 4010; Costech Analytical Technologies, Inc.) coupled to a Delta V Plus (Thermo Scientific, Inc.) with a Conflo IV (Thermo Scientific, Inc.). Values of $\delta^{13}C_{org}$ were calculated relative to the international Pee Dee Belemnite (PDB) standard (Craig 1957) with a precision of ± 0.2‰, whereas $\delta^{15}N_{org}$ values were calculated relative to the atmospheric nitrogen (AIR) standard (Mariotti 1983) with a precision of ± 0.3‰. Values for N-wt% and C-wt% were calculated using the linear relationship between m/z 28 and m/z 44 beam areas and standards of known N-wt% and C-wt%, respectively. N-wt% and C-wt% were measured with the ECS 4010 using a thermal conductivity detector.

Results

Miocene–Pliocene Aquifer shallow sediment stratigraphy

The sediment cores (4 m) recovered at the intertidal zone of each study site revealed large compositional differences in the shallow coastal sediments. On the east shore of Mobile Bay we identified the presence of a fine-grained and organic-rich sediment layer (hereafter referred to as peat layer) that has moderate hydraulic conductivity (8.2 m day^{-1}) (Figs. 2, 3). On the southeastern shore, the sediment core TS-SE collected at the intertidal zone revealed from top to bottom: a coarse beach sand layer (A) of 0.5 m

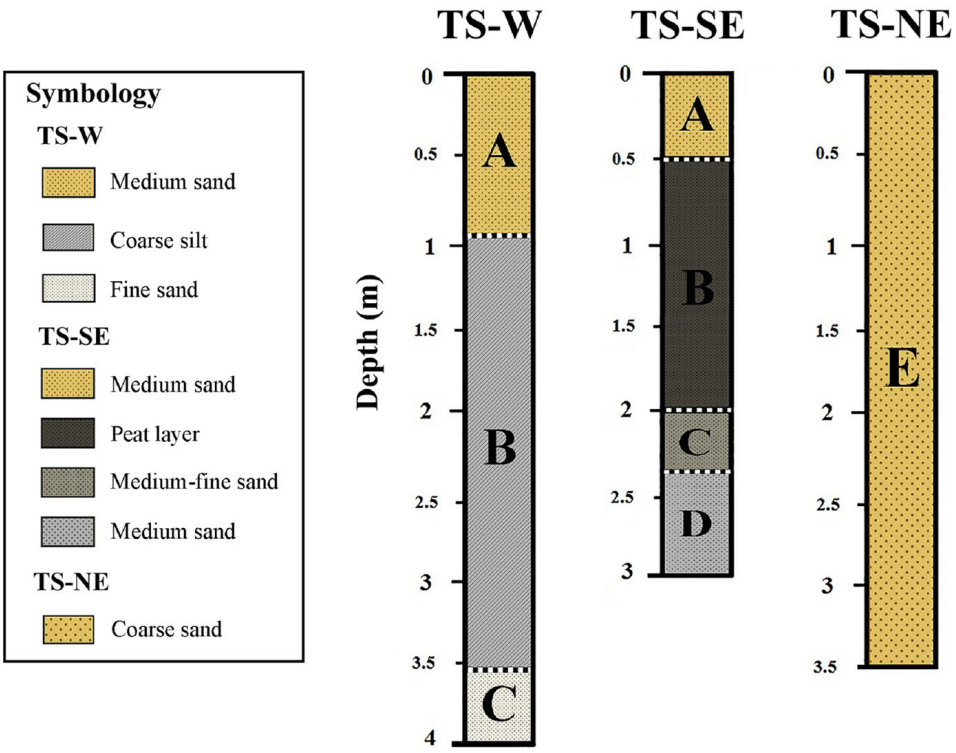

Fig. 3 Sediment cores collected at study site TS-W on the western shore, TS-SE on the southeastern shore, and TS-NE in the northeastern shore from locations indicated in Fig. 2

thickness and 3% organic matter content, underlain by a 1.5-m organic-rich black fine sand (B) with an organic matter content of up to 36% (peat layer), which was in contact with the Miocene–Pliocene Aquifer (layers C and D) with an organic matter content of 2–7% (Figs. 2b, 3). Additional cores collected (n = 5) on both the southeastern and northeastern shores showed that the presence and composition of the peat layer varies significantly, with organic matter content varying from 15% to a maximum of 36%. On the northeastern shore, sediment core TS-NE collected at the intertidal zone of study site TS-NE showed no vertical structure, consisting exclusively of coarse sand (E), that was artificially added to develop beach areas (Figs. 2c, 3). In contrast, on the western shore, the peat layer was absent in sediment core TS-W collected at the intertidal zone of study site TS-W. From top to bottom, core TS-W was comprised of a 0.8 m coarse beach sand (A) with only 2% organic matter, underlain by a 2.5-m thick silt layer (B) with 11% of organic matter and very low hydraulic conductivity (4.1 m day^{-1}), and a 0.5-m fine sand layer (C) with 5% organic matter (Figs. 2a, 3).

Analyses of the organic matter from the peat layer (B) in sediment core TS-SE revealed a large range of carbon and nitrogen weight content. The C-wt% ranged between 0.43% at a depth of 90–100 cm and 6.15% at 65 cm, with an average of 3.36 ± 2.15%, whereas the N-wt% was highest at 45 cm with 0.12% and lowest at 70 cm with 0.33%, with an average of 0.25 ± 0.07% (Table 1). The average C/N ratio was 19.0 ± 2.4, ranging between 16.8 at 55 cm and 24.4 at 45 cm. Both stable isotopes $\delta^{13}C_{org}$ and $\delta^{15}N_{org}$ were highest ($\delta^{13}C_{org}$ = − 24 to − 23‰, $\delta^{15}N_{org}$ = 3 to 4‰) at a depth of 50–60 cm and were lowest ($\delta^{13}C_{org}$ = − 30 to − 28‰, $\delta^{15}N_{org}$ = 0 to 1‰) at 80–90 cm (Fig. 4). The $\delta^{13}C_{org}$ values were on average − 25.7 ± 0.3‰, ranging from − 29.4 ± 0.1‰ at 85 cm and − 23.3 ± 0.3‰ at 55 cm, compared to the average $\delta^{15}N_{org}$ in this layer of 2.1 ± 0.2, with a minimum value of 0.4 ± 0.2‰ at 80 cm and a maximum of 3.8 ± 0.1‰ at 50 cm (Table 1).

Surface (river and bay) and groundwater compositions

Groundwater DO, nutrient concentrations (NO_3^-, NH_4^+, DON, and PO_4^{3-}), $\delta^{15}N_{NO_3}$, $\delta^{18}O_{NO_3}$, DOC concentrations, and DOM compositions varied significantly both spatially (between study sites) and temporally (during dry and wet seasons). However, although we also found significant spatial variations in

Table 1 Characterization of the organic matter present in the peat layer (B) analyzed from sediment core TS-SE, showing C-weight percent, N-weight percent, C/N ratio, stable isotopes $\delta^{13}C_{org}$ and $\delta^{15}N_{org}$

Cores present	Layer ID	Depth (cm)	C-weight percent (%)	$\delta^{13}C_{org}$ (‰ PDB)	N-weight percent (%)	$\delta^{15}N_{org}$ (‰ AIR)	C/N in sediment
TS-SE	B	45	2.88	− 27.7 ± 0.2	0.12	2.0 ± 0.1	24.4
		50	5.28	− 23.7 ± 0.1	0.31	3.8 ± 0.1	17.1
		55	4.97	− 23.3 ± 0.3	0.30	3.7 ± 0.2	16.8
		60	4.99	− 23.4 ± 0.1	0.29	2.6 ± 0.1	17.1
		65	6.15	− 24.4 ± 0.1	0.29	1.3 ± 0.1	21.0
		70	5.98	− 24.6 ± 0.1	0.33	1.5 ± 0.1	18.2
		75	4.41	− 24.4 ± 0.2	0.24	1.4 ± 0.1	18.0
		80	3.29	− 24.9 ± 0.1	0.17	0.4 ± 0.2	19.6
		85	1.03	− 29.4 ± 0.1	–	–	–
		90	0.50	− 28.7 ± 0.4	–	–	–
		95	0.43	− 25.0 ± 0.1	–	–	–
		100	0.43	− 28.3 ± 0.1	–	–	–
Average			3.36	− 25.7 ± 0.3	0.26	2.1 ± 0.2	19.0

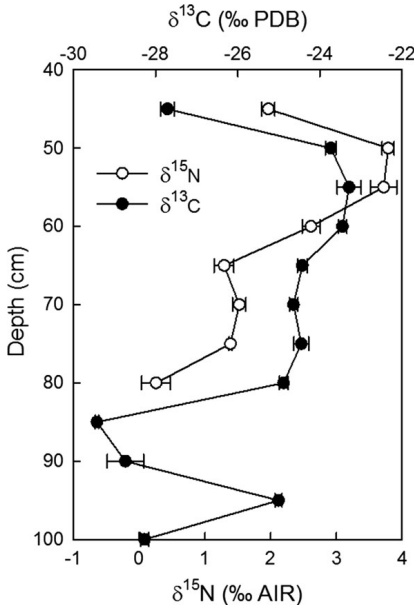

Fig. 4 Vertical profile of stable isotopes $\delta^{13}C$ and $\delta^{15}N$ of the organic matter present in the peat layer (B) analyzed from sediment core TS-SE. Both $\delta^{13}C_{org}$ and $\delta^{15}N_{org}$ were highest ($\delta^{13}C$ = − 24 to − 23‰, $\delta^{15}N$ = 3 to 4‰) at a depth of 50–60 cm and were lowest ($\delta^{13}C$ = − 30 to − 28‰, $\delta^{15}N$ = 0 to 1‰) at 80–90 cm

the composition of Mobile Bay receiving surface water between study sites, we did not detect large seasonal variations (Table 1 in Online Appendix). A detailed summary of the surface and groundwater compositions during the dry and wet seasons can be found in Table 2 and in the following subsections.

Dissolved oxygen (DO) levels

As to be expected, the highest DO values of 6–8 mg L^{-1} in Mobile Bay surface waters were measured near the river inlet (Mobile–Tensaw River Delta) and the estuary outlet to the GOM (Main Pass). During our study, DO in Mobile Bay waters along the east shore was always below 2 mg L^{-1} (Fig. 1 in Online Appendix). Considering the whole bay, the overall average DO concentration during all sampling campaigns was 4.1 ± 1.4 mg L^{-1} (n = 88) (Table 2). In the Mobile–Tensaw River System DO was on average 7.0 ± 1.8 mg L^{-1} (n = 18) combining all sampling campaigns, ranging between 5.4 and 10 mg L^{-1} (Table 2).

DO in groundwater on the western shore was on average 1.2 ± 0.3 mg L^{-1} (n = 3) in the inland wells (W-Well-1–3), whereas in the intertidal piezometers (W-Pz-1–5) DO was 2.1 ± 1.0 mg L^{-1} (n = 18) (Fig. 5). On the southeastern shore, DO was significantly higher in groundwater collected from the inland wells SE-Well-1 and -2 with an average of 5.6 ± 0.7 mg L^{-1} (n = 9). In contrast, DO in groundwater from the intertidal piezometers (SE-Pz-1–5) was on average 0.8 ± 0.7 mg L^{-1} (n = 27) (Fig. 5). In the

Table 2 Average composition (NO_3^-, NH_4^+, DON, PO_4^{3-}, N/P, $\delta^{15}N_{NO_3}$ and $\delta^{18}O_{NO_3}$, DOC, and DOM) of Mobile Bay surface water, river water, and groundwater during the dry and wet seasons and during all sampling campaigns ("overall")

	Location	Season	DO (mg L^{-1})	NO_3^- (mmol m^{-3})	NH_4^+	DON	PO_4^{3-}	N/P	$\delta^{15}N_{NO_3}$ (‰)	$\delta^{18}O_{NO_3}$	DOC (mmol m^{-3})	DOM		
												C1 (%)	C2 (%)	C3 (%)
Mobile Bay		Overall	4.1 ± 1.4	4.5 ± 1.7	2.6 ± 1.2	26 ± 9.8	0.4 ± 0.1	16 ± 11	12 ± 4	17 ± 6	520 ± 320	28 ± 7	33 ± 7	37 ± 12
		Dry	3.1 ± 1.0	4.0 ± 1.0	2.9 ± 1.3	24 ± 9.2	0.3 ± 0.1	17 ± 11	12 ± 3	16 ± 5	340 ± 210	29 ± 7	35 ± 8	33 ± 11
		Wet	4.8 ± 1.6	4.9 ± 2.5	2.2 ± 1.0	27 ± 9.5	0.4 ± 0.1	14 ± 8	13 ± 4	18 ± 6	570 ± 390	26 ± 6	31 ± 6	41 ± 14
Rivers		Overall	7.0 ± 1.8	8.4 ± 2.0	5.1 ± 1.7	30 ± 8.1	0.8 ± 0.3	21 ± 10	5 ± 1	6 ± 2	570 ± 83	26 ± 4	41 ± 3	33 ± 6
		Dry	7.1 ± 1.7	8.9 ± 2.4	4.0 ± 1.3	31 ± 10	1.0 ± 0.3	18 ± 4	4 ± 1	7 ± 2	470 ± 33	28 ± 1	44 ± 1	28 ± 1
		Wet	6.9 ± 2.0	7.4 ± 1.5	7.0 ± 2.0	29 ± 6.3	0.3 ± 0.1	30 ± 12	6 ± 1	5 ± 1	640 ± 25	25 ± 4	38 ± 1	37 ± 5
Groundwater	W inland wells	Overall	1.2 ± 0.3	96 ± 23	2.1 ± 0.7	10 ± 4.5	0.1 ± 0.03	870 ± 220	7 ± 3	6 ± 2	–	–	–	–
		Dry	1.2 ± 0.3	64 ± 15	2.6 ± 0.9	16 ± 7.2	0.1 ± 0.03	790 ± 190	9 ± 3	7 ± 1	–	–	–	–
		Wet	1.2 ± 0.3	120 ± 29	1.0 ± 0.4	6.0 ± 2.7	0.1 ± 0.03	1200 ± 290	4 ± 2	6 ± 1	–	–	–	–
	W intertidal piezometers	Overall	2.1 ± 1.0	4.5 ± 1.5	3.8 ± 2.1	25 ± 12	0.1 ± 0.08	79 ± 23	7 ± 3	24 ± 8	160 ± 67	11 ± 1	0	89 ± 1
		Dry	1.2 ± 0.8	6.7 ± 2.1	4.5 ± 1.9	28 ± 13	0.1 ± 0.1	70 ± 30	8 ± 3	27 ± 10	220 ± 8.0	11 ± 1	0	89 ± 1
		Wet	2.4 ± 1.0	2.4 ± 0.9	2.2 ± 1.0	20 ± 4.9	0.1 ± 0.02	29 ± 12	6 ± 2	19 ± 6	130 ± 25	11 ± 1	0	89 ± 1
	SE inland wells	Overall	5.6 ± 0.7	110 ± 34	4.3 ± 1.3	80 ± 45	0.1 ± 0.04	1200 ± 490	15 ± 8	8 ± 2	–	–	–	–
		Dry	4.8 ± 0.6	110 ± 30	7.5 ± 2.2	110 ± 65	0.2 ± 0.05	1100 ± 580	28 ± 15	9 ± 2	–	–	–	–
		Wet	6.2 ± 0.7	110 ± 40	1.1 ± 0.4	50 ± 34	0.1 ± 0.01	990 ± 490	3 ± 1	6 ± 1	–	–	–	–
	SE intertidal piezometers	Overall	0.8 ± 0.7	14 ± 5.7	108 ± 35	94 ± 20	0.7 ± 0.3	250 ± 120	11 ± 4	18 ± 6	830 ± 410	17 ± 12	19 ± 21	63 ± 32
		Dry	0.6 ± 0.3	8.0 ± 3.4	140 ± 50	130 ± 34	0.5 ± 0.2	230 ± 190	10 ± 4	23 ± 8	1000 ± 430	22 ± 13	29 ± 19	48 ± 21
		Wet	0.9 ± 0.8	20 ± 8.0	75 ± 20	58 ± 22	0.9 ± 0.4	330 ± 210	11 ± 2	14 ± 4	792 ± 410	10 ± 1	1 ± 1	89 ± 1
	NE intertidal piezometers	Overall	2.2 ± 1.0	19 ± 9.0	7.0 ± 2.5	24 ± 8.0	0.3 ± 0.1	66 ± 29	7 ± 2	12 ± 5	120 ± 25	9 ± 1	1 ± 1	90 ± 1
		Dry	1.3 ± 0.8	13 ± 5.0	8.0 ± 3.1	32 ± 12	0.5 ± 0.2	26 ± 10	7 ± 2	13 ± 5	–	–	–	–
		Wet	2.4 ± 1.0	30 ± 10	6.0 ± 2.5	16 ± 4.9	0.2 ± 0.1	170 ± 85	7 ± 2	10 ± 3	120 ± 25	9 ± 1	1 ± 1	90 ± 1

For groundwater samples an average is provided at study site TS-W on the western shore from the inland wells ("W inland wells") and the intertidal piezometers ("W intertidal piezometers"), at TS-SE on the southeastern shore ("SE inland wells" and "SE intertidal piezometers"), and TS-NE on the northeastern shore ("NE inland wells" and "NE intertidal piezometers")

northeastern shore the overall average groundwater DO concentration in the intertidal piezometers (NE-Pz-1–5) was 2.2 ± 1.0 mg L^{-1} (n = 17) (Table 2).

Nitrate (NO_3^-) concentrations

The average NO_3^- concentration in surface waters of Mobile Bay during all sampling campaigns was 4.5 ± 1.7 mmol m^{-3} (n = 82) (Table 2). The highest NO_3^- concentrations were measured along the northeastern shore and the northern sector of the bay near the river delta and were between 6.0 and 22 mmol m^{-3} and lowest were in Bon Secour Bay between 0.7 and 0.9 mmol m^{-3} (Fig. 2a in Online Appendix). In the Mobile–Tensaw River System the average NO_3^- concentration was 8.4 ± 2.0 mmol m^{-3} (n = 23) (Table 2).

On the western shore, the average NO_3^- concentration in groundwater was 96 ± 23 mmol m^{-3} (n = 3) in the inland wells, which is much higher than the average NO_3^- concentration measured in the shallow intertidal zone piezometers of 4.5 ± 1.5 mmol m^{-3} (n = 14). Similarly, on the southeastern shore NO_3^- was higher in the inland wells with an average concentration of 110 ± 34 mmol m^{-3} (n = 8), whereas in the

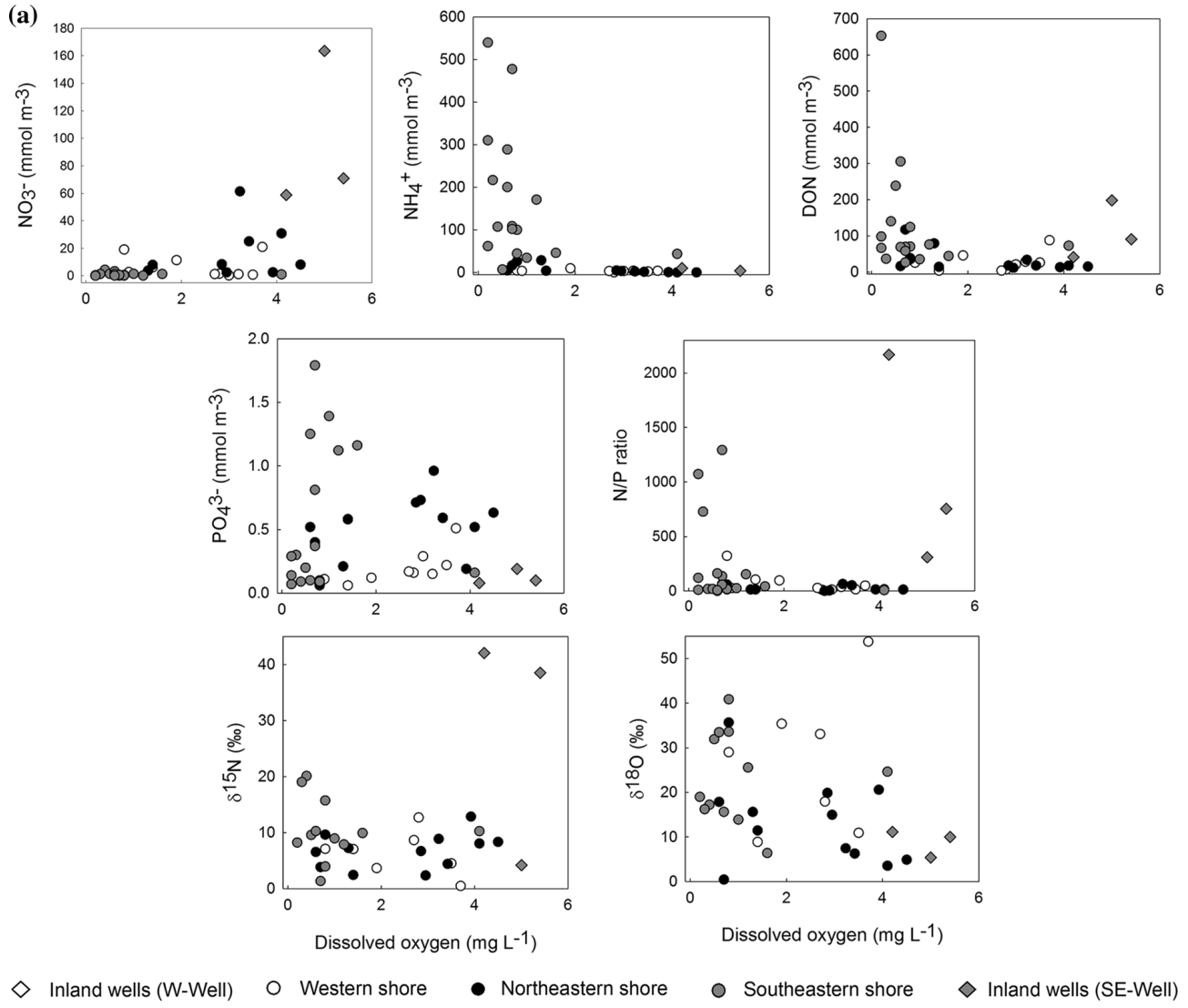

Fig. 5 Groundwater dissolved oxygen (DO), NO_3^-, NH_4^+, DON, and PO_4^{3-} concentrations, N/P molar ratio, and nitrate stable isotopes ($\delta^{15}N_{NO_3}$ and $\delta^{18}O_{NO_3}$) values in the inland wells and the intertidal piezometers during the dry (**a**) and wet (**b**) seasons. Most groundwater samples collected form the peat layer showed anoxic conditions (DO < 1 mg L^{-1}) and significantly higher NH_4^+, DON, and PO_4^{3-} compared to the other study sites

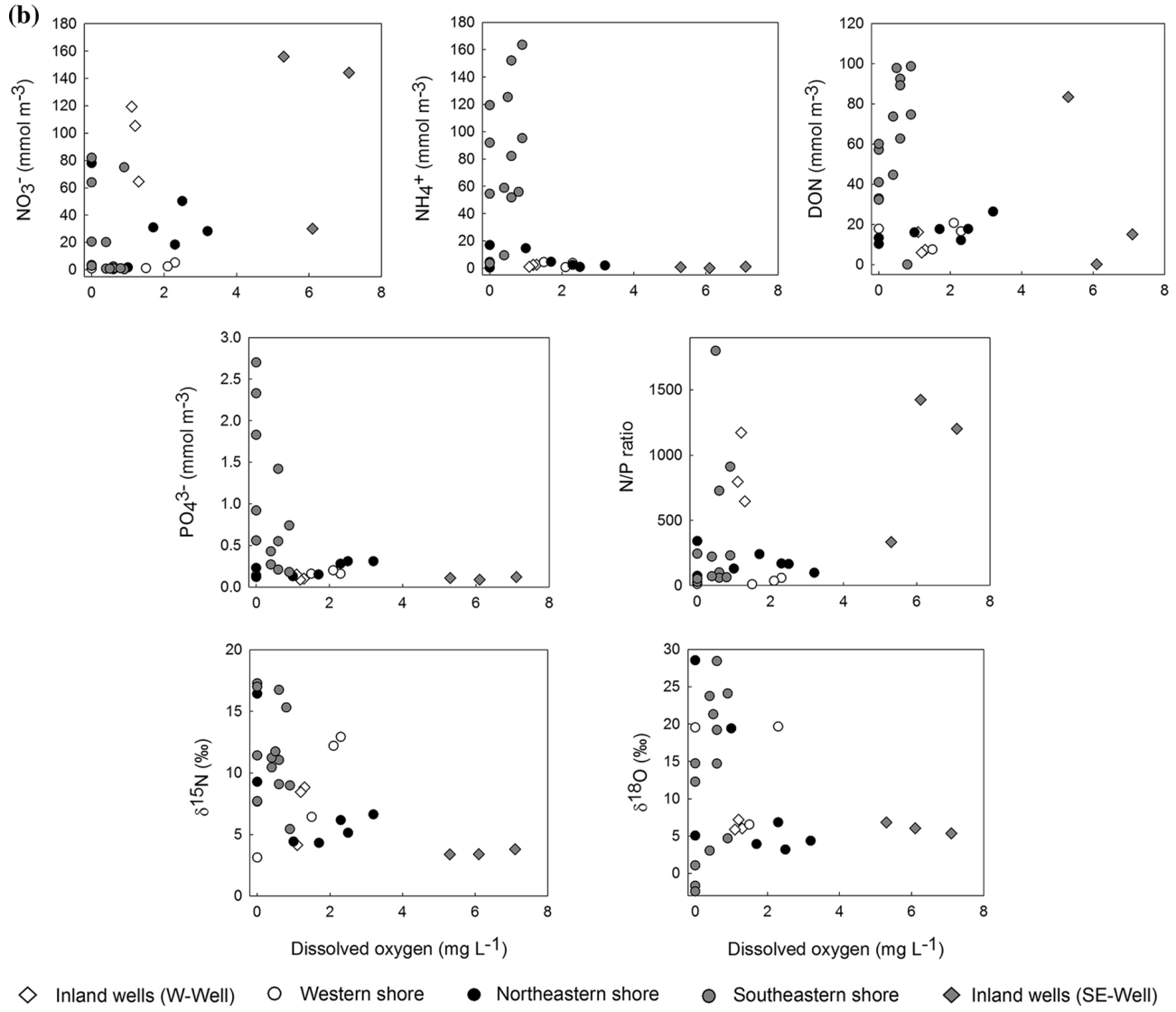

Fig. 5 continued

intertidal piezometers the average NO_3^- concentration was 14 ± 5.7 (n = 32). On the northeastern shore, the average NO_3^- in the intertidal piezometers was 19 ± 9.0 mmol m^{-3} (n = 19) (Fig. 5; Table 2).

Ammonium (NH_4^+) concentrations

During this study the average NH_4^+ concentration in Mobile Bay surface water was 2.6 ± 1.2 mmol m^{-3} (n = 82) (Table 2). We found the highest NH_4^+ concentration (between 8.0 and 11 mmol m^{-3}) on the southeastern shore, and lowest in Bon Secour Bay and near the river delta (0.3–0.7 mmol m^{-3}) (Fig. 2b in Online Appendix). In the Mobile–Tensaw River System NH_4^+ was on average 5.1 ± 1.7 mmol m^{-3} (n = 23) (Table 2).

Specifically, on the western shore at study site TS-W the average groundwater NH_4^+ concentration in the inland wells was 2.1 ± 0.7 mmol m^{-3} (n = 3) and was similar to the intertidal piezometers with 3.8 ± 2.1 mmol m^{-3} (n = 14). For comparison, on the southeastern shore, NH_4^+ in the inland wells was on average 4.3 ± 1.3 mmol m^{-3} (n = 8) and was 108 ± 35 mmol m^{-3} (n = 32) in the intertidal piezometers. On the northeastern shore intertidal piezometers, NH_4^+ was on average 7.0 ± 2.5 mmol m^{-3} (n = 19) (Fig. 5; Table 2).

Dissolved organic nitrogen (DON) concentrations

During this study the average DON concentrations in Mobile Bay surface water was 26 ± 9.8 mmol m^{-3} (n = 82) (Table 2). Elevated levels of DON concentrations were always detected in Bon Secour Bay (36 ± 11 mmol m^{-3}) and the northeastern shore (32 mmol m^{-3}). Compared to this part of Mobile Bay, DON along the southeastern was 24 ± 6.1 mmol m^{-3} and along the western (20 ± 6.4 mmol m^{-3}) shores (Fig. 2c in Online Appendix). In the Mobile–Tensaw River System the average DON concentration was 30 ± 10 mmol m^{-3} (n = 23) (Table 2).

The average DON concentration in groundwater on the western shore was 10 ± 4 mmol m^{-3} (n = 3) in the inland wells and was 25 ± 12 mmol m^{-3} (n = 14) in the intertidal piezometers. The highest DON concentrations were measured on the southeastern shore where the average DON concentration in groundwater of the inland wells was 80 ± 45 mmol m^{-3} (n = 8) compared to the average of 94 ± 20 mmol m^{-3} (n = 32) measured in the intertidal piezometers. On the northeastern shore we found that DON in groundwater in the intertidal piezometers was 24 ± 8 mmol m^{-3} (n = 19) (Fig. 5; Table 2).

Phosphorous (as reactive PO_4^{3-}) concentrations

The average PO_4^{3-} concentration in Mobile Bay during all sampling campaigns was 0.4 ± 0.1 mmol m^{-3} (n = 82) (Table 2). The highest PO_4^{3-} concentrations were found on the northeastern shore and near the river delta with values of 0.5–1.4 mmol m^{-3}, and were lowest along the western shore and Bon Secour Bay with concentrations of 0.1–0.3 mmol m^{-3} (Fig. 2d in Online Appendix). In the Mobile–Tensaw River System PO_4^{3-} was on average 0.8 ± 0.3 mmol m^{-3} (n = 23) (Table 2).

On the western shore the average PO_4^{3-} concentration was similar in the inland wells 0.1 ± 0.08 mmol m^{-3} (n = 3) and the intertidal piezometers 0.2 ± 0.04 mmol m^{-3} (n = 14). These concentrations were also very similar to the observed PO_4^{3-} levels on the southeastern shore, where the average PO_4^{3-} in groundwater was 0.1 ± 0.04 mmol m^{-3} (n = 8) in the inland wells and 0.7 ± 0.3 mmol m^{-3} (n = 32) in the intertidal piezometers. The average PO_4^{3-} concentration in groundwater from the intertidal piezometers installed on the northeastern shore of Mobile Bay was 0.3 ± 0.1 mmol m^{-3} (n = 19) (Fig. 5; Table 2).

Inorganic N/P ratio (calculated as $NO_3^- + NH_4^+/PO_4^{3-}$)

The highest N/P ratios in Mobile Bay were found along the southeastern and western shores with average values of 20 ± 5.2 and 60 ± 12, respectively, whereas the minimum values were found in Bon Secour Bay with an average of 6.4 ± 1.6. The overall average N/P ratio in Mobile Bay surface water during this study was 16 ± 11 (n = 82) (Fig. 2e in Online Appendix). The Mobile–Tensaw River System N/P ratio was on average 21 ± 10 (n = 23) (Table 2).

The N/P ratios in groundwater were significantly higher in the inland wells compared to the intertidal piezometers at all study sites. In the inland wells located on the western and southeastern shores N/P was on average 870 ± 220 (n = 3) and 1200 ± 490 (n = 8), respectively. In the intertidal piezometers of the western, southeastern, and northeastern shores the average N/P ratios were 79 ± 23 (n = 14), 250 ± 120 (n = 32), and 66 ± 29 (n = 19) (Fig. 5; Table 2).

NO_3^- stable isotopes ($\delta^{15}N_{NO_3}$ and $\delta^{18}O_{NO_3}$)

During this study, the $\delta^{15}N_{NO_3}$ and $\delta^{18}O_{NO_3}$ in Mobile Bay surface water were on average 12 ± 4‰ and 17 ± 6‰ (n = 54), respectively. Both isotopes were highest in the southern sector of the bay, specifically in Bon Secour Bay, with values of 16–27‰ and were lower near the river delta with values of 6–10‰ and 4–11‰, respectively (Fig. 3a, b in Online Appendix). The average $\delta^{15}N_{NO_3}$ and $\delta^{18}O_{NO_3}$ in the Mobile–Tensaw River System were 5 ± 1‰ and 6 ± 2‰ (n = 16), respectively (Table 2).

On the western shore, the groundwater $\delta^{15}N_{NO_3}$ values were similar both in inland wells and intertidal piezometers with an overall average of 7 ± 3‰ (n = 15). However, we found almost double values on the southeastern shore, the overall $\delta^{15}N_{NO_3}$ average in the inland wells was 15 ± 8‰ (n = 6), whereas in the intertidal piezometers $\delta^{15}N_{NO_3}$ was 11 ± 4‰ (n = 26). On the northeastern shore the average $\delta^{15}N_{NO_3}$ in the intertidal piezometers was 7 ± 2‰

(n = 19). The $\delta^{18}O_{NO_3}$ values were generally lower in the inland wells of the western shore with an average of 6 ± 2‰ (n = 3) compared to the intertidal piezometers where $\delta^{18}O_{NO_3}$ was 24 ± 8‰ (n = 12). In the inland wells of the southeastern shore at study site TS-SE the average $\delta^{18}O_{NO_3}$ was 8 ± 2‰ (n = 6) and was 18 ± 6‰ (n = 26) in the intertidal piezometers. On the northeastern shore the average $\delta^{18}O_{NO_3}$ in the intertidal piezometers was 12 ± 5‰ (n = 19) (Fig. 5; Table 2).

Dissolved organic carbon (DOC) concentrations

DOC concentrations in Mobile Bay during all sampling campaigns were on average 520 ± 320 mmol m^{-3} (n = 30). The highest DOC was measured along the northeastern shore and Bon Secour Bay with values ranging from 540 to 1250 mmol m^{-3}, whereas the lowest concentrations were measured near the river delta and the western shore where DOC was relatively constant between 230 and 370 mmol m^{-3} (Fig. 4 in Online Appendix). Similarly, we did not find large variations of DOC in the Mobile–Tensaw River System, with an average concentration during this study of 570 ± 83 mmol m^{-3} (n = 5) (Table 2).

The average DOC concentration in groundwater recovered from the intertidal piezometers of the western shore was 160 ± 70 mmol m^{-3} (n = 4). On the southeastern shore the groundwater DOC concentration in the intertidal piezometers was significantly higher with an average of 830 ± 410 mmol m^{-3} (n = 14), whereas in the northeastern shore was 120 ± 25 mmol m^{-3} (n = 5) (Table 2).

Dissolved organic matter (DOM) composition

In all water samples DOM analyses revealed three groups of organic compounds (referred hereafter as components C1, C2, and C3). The excitation–emission maxima were 255–456 nm for C1, 310, 386 nm for C2, and 280–320 nm for C3. C1 and C2 were assigned as refractory humic-like compounds from decaying plant material. In contrast, C3 was assigned as more labile protein-like (tyrosine) DOM compounds sourced from aquatic microorganisms.

The average percentages of C1, C2, and C3 in Mobile Bay were present in similar proportions during all sampling campaigns with values of 28 ± 7% (C1), 33 ± 7% (C2), and 37 ± 12% (C3) (n = 31). However, the percentage of humic-like C1 and C2 were higher near the river delta and in Bon Secour Bay and on the northeastern shore with values of 26–46% (Fig. 5a, b in Online Appendix). The spatial distribution of protein-like C3 showed nearly the opposite trend, being highest in the mid-bay area (35–65%) and lower near the river delta, the northeastern shore and Bon Secour Bay (20–25%) (Fig. 5c in Online Appendix). In surface water from the Mobile–Tensaw River System the predominant DOM component was C2 with 41 ± 3%, whereas C3 and C1 were on average 33 ± 6% and 26 ± 4%, respectively (n = 5) (Table 2).

In groundwater collected from the intertidal piezometers of the western shore, protein-like C3 was the major DOM component with an average of 89 ± 1%, while the remaining 11 ± 1% corresponded with C1 (n = 4). On the southeastern shore, C3 was also the major DOM component in groundwater with an average of 89 ± 2% in piezometers SE-Pz-1 to -5, being C1 an average of 9 ± 1% (n = 8). However, in the multi-level piezometer SE-Pz-4.5 installed in the peat layer on the southeastern shore, the humic-like C2 was the major component with an average of 43 ± 4%, while humic-like C1 and protein-like C3 represented 29 ± 10% and 28 ± 12% (n = 6), respectively. On the northeastern shore, protein-like C3 was the major DOM component in groundwater with an average of 89 ± 1%, while humic-like C1 and C2 represented 10 ± 1% and 1 ± 1% (n = 5), respectively (Table 2).

Microbial community composition and metabolic pathways in groundwater

In groundwater collected from the inland well SE-Well-2 on the east shore, aerobic facultative freshwater genera *Acinetobacter*, *Catenococcus*, *Vogesella*, *Rheinheimera*, *Sphingomonas*, and *Nitrospira* (*Gammaproteobacteria* and *Alphaproteobacteria* classes) were the most frequent taxa found in the samples (Table 2 in Online Appendix). The main metabolic pathways of these bacteria in the inland groundwater were aerobic organic matter mineralization (*Vogesella*, *Sphingomonas*, and *Acinetobacter*), nitrification (*Nitrospira*), and sulfur reduction (*Catenococcus*) (Table 2 in Online Appendix).

In groundwater samples collected from the intertidal piezometers installed in the peat layer on the east shore (SE-Pz-1 and -4.5-A to -4.5-F), the microbial taxa with highest relative proportion were *Deltaproteobacteria*, *Anaerolineae*, *Dehalococcoidia*, *Thermodesulfovibrionia*, and *Actinobacteria.* The most abundant genera from class *Deltaproteobacteria* (i.e. *Geobacter*, *Desulfobacca*, and *Desulfatiglans*) are NO_3^-, sulfate (SO_4^{2-}), and ferrous iron (Fe^{2+}) reducers, while classes *Dehalococcoidia* and *Anaerolineae* consist of genera that are capable of implementing organic matter mineralization as fermenters and hydrolyzers. High sequence proportions of methanogenic archaea (genera *Methanoregula* and *Methanolinea*) were also observed in samples SE-Pz-1, -4.5-C, and -4.5-D (Table 2 in Online Appendix).

In groundwater recovered from the intertidal piezometers of the northeastern shore (NE-Pz-1A, NE-Pz-1B, and EN-Pz-5) the dominant genera from class *Gammaproteobacteria* were methane oxidizing bacteria *Methylobacter*, *Methylococcus*, and *Sporosarcina*. These methanotrophs were not found in any other samples (Table 2 in Online Appendix).

Nutrient fluxes via SGD and river discharge

Using the SGD rates reported in Montiel et al. (2018) obtained during the dry and wet seasons and using the site-specific and season specific nutrient concentrations presented here, we calculated the SGD-derived nutrients fluxes at the three study sites of Mobile Bay. All nutrient fluxes were calculated by multiplying the site-specific SGD rates by the corresponding nutrients concentrations as shown in Table 3.

On the western shore, during the dry season we obtained an SGD-NO_3^- flux of 5.8×10^5 mmol day^{-1}, an SGD-NH_4^+ flux of $8.1 \pm 2.7 \times 10^5$ mmol day^{-1}, an SGD-DON flux of $48 \pm 14 \times 10^5$ mmol day^{-1}, an SGD-PO_4^{3-} flux of $0.2 \pm 0.08 \times 10^5$ mmol day^{-1}, and an SGD-DOC flux of $310 \pm 100 \times 10^5$ mmol day^{-1} (Fig. 6a; Table 2). During the wet season, we found an SGD-NO_3^- flux of $12 \pm 4.0 \times 10^5$ mmol day^{-1}, an SGD-NH_4^+ flux of $4.8 \pm 1.4 \times 10^5$ mmol day^{-1}, an SGD-DON flux of $50 \pm 17 \times 10^5$ mmol day^{-1}, an SGD-PO_4^{3-} flux of $0.4 \pm 0.1 \times 10^5$ mmol day^{-1}, and an SGD-DOC flux of $400 \pm 140 \times 10^5$ mmol day^{-1} (Fig. 6b; Table 3).

On the southeastern shore, during the dry season we obtained an SGD-NO_3^- flux of $18 \pm 8.1 \times 10^5$ mmol day^{-1}, an SGD-NH_4^+ flux of $320 \pm 140 \times 10^5$ mmol day^{-1}, an SGD-DON flux of $300 \pm 130 \times 10^5$ mmol day^{-1}, an SGD-PO_4^{3-} flux of $1.1 \pm 0.5 \times 10^5$ mmol day^{-1}, and an SGD-DOC flux of $2300 \pm 990 \times 10^5$ mmol day^{-1} (Fig. 6a; Table 3). During the wet season we found an SGD-NO_3^- flux of $74 \pm 35 \times 10^5$ mmol day^{-1}, an SGD-NH_4^+ flux of $290 \pm 130 \times 10^5$ mmol day^{-1}, an SGD-DON flux of $220 \pm 100 \times 10^5$ mmol day^{-1}, an SGD-PO_4^{3-} flux of $3.4 \pm 1.6 \times 10^5$ mmol day^{-1}, and an SGD-DOC flux of $3000 \pm 1000 \times 10^5$ mmol day^{-1} (Fig. 6b; Table 3).

On the northeastern shore during the dry season we found an SGD-NO_3^- flux of $50 \pm 21 \times 10^5$ mmol day^{-1}, an SGD-NH_4^+ flux of $31 \pm 14 \times 10^5$ mmol day^{-1}, an SGD-DON flux of $120 \pm 54 \times 10^5$ mmol day^{-1}, an SGD-PO_4^{3-} flux of $1.9 \pm 0.8 \times 10^5$ mmol day^{-1}, and an SGD-DOC flux of $470 \pm 200 \times 10^5$ mmol day^{-1} (Fig. 6a; Table 3). During the wet season we obtained an SGD-NO_3^- flux of $170 \pm 63 \times 10^5$ mmol day^{-1}, an SGD-NH_4^+ flux of $34 \pm 13 \times 10^5$ mmol day^{-1}, an SGD-DON flux of $90 \pm 34 \times 10^5$ mmol day^{-1}, an SGD-PO_4^{3-} flux of $1.1 \pm 0.7 \times 10^5$ mmol day^{-1}, and an SGD-DOC flux of $680 \pm 230 \times 10^5$ mmol day^{-1} (Fig. 6b; Table 3).

During this study, the Mobile–Tensaw River System discharge ranged largely; it was 70×10^5 m^3 day^{-1} during the dry season and 1700×10^5 m^3 dAY^{-1} during wet season (https://waterwatch.usgs.gov). Using the rivers discharge and corresponding nutrients concentrations during the wet season, we obtained a river NO_3^- flux of $13{,}000 \pm 1100 \times 10^5$ mmol day^{-1}, a NH_4^+ flux of $12{,}000 \pm 1100 \times 10^5$ mmol day^{-1}, a DON flux of $49{,}000 \pm 4300 \times 10^5$ mmol day^{-1}, a PO_4^{3-} flux of $510 \pm 180 \times 10^5$ mmol day^{-1}, and a SGD-DOC flux of $1{,}100{,}000 \pm 370{,}000 \times 10^5$ mmol day^{-1} (Fig. 6a, b; Table 3). During the dry season we found a riverine NO_3^- flux of $620 \pm 220 \times 10^5$ mmol day^{-1}, a NH_4^+ flux of $280 \pm 100 \times 10^5$ mmol day^{-1}, a DON flux of $2200 \pm 770 \times 10^5$ mmol day^{-1}, a PO_4^{3-} flux of $70 \pm 30 \times 10^5$ mmol day^{-1}, and a SGD-DOC flux of $33{,}000 \pm 14{,}000 \times 10^5$ mmol day^{-1} (Fig. 6a, b; Table 3).

Table 3 All values utilized to evaluate the river- and SGD-derived nutrient (NO_3^-, NH_4^+, DON and PO_4^{3-}) fluxes on the western, southeastern, and northeastern shores in Mobile Bay

	Discharge (dry–wet) ($\times 10^5$ m^3 day^{-1})	NO_3^-	NH_4^+	DON	PO_4^{3-}	NO_3^-	NH_4^+	DON	PO_4^{3-}	Mobile Bay nutrients loading (%)
		Average concentration (dry–wet) (mmol m^{-3})				Nutrient fluxes (dry–wet) $\times 10^5$ mmol day^{-1} ($\times 10^6$ mol $year^{-1}$)				
Western shore SGD	1.8–2.4	6.7–2.4	4.5–2.0	28–20	0.2–0.1	12 (0.4)–5.8 (0.2)	8.1 (0.3)–4.8 (0.2)	50 (0.2)–48 (0.2)	0.4 (0.01)–0.2 (0.01)	NO_3^- = 1.7–0.1 NH_4^+ = 1.3–0.1 DON = 1.9–0.1 PO_4^{3-} = 0.4–0.1
Southeastern shore SGD	2.3–3.8	8.0–20	140–75	130–60	0.5–0.9	18 (0.7)–74 (2.7)	320 (12)–290 (10)	300 (11)–220 (8.0)	1.1 (0.04)–3.4 (0.03)	NO_3^- = 2.6–0.6 NH_4^+ = 50–2.3 DON = 12–0.4 PO_4^{3-} = 1.4–0.6
Northeastern shore SGD	3.9–5.7	13–30	8.0–6.0	32–16	0.5–0.2	50 (1.8)–170 (6.3)	31 (1.1)–34 (1.2)	120 (1.1)–90 (0.8)	1.9 (0.7)–1.1 (0.4)	NO_3^- = 7.1–1.3 NH_4^+ = 4.9–0.3 DON = 4.7–0.2 PO_4^{3-} = 2.3–0.2
Total SGD	8.0–12	N/A	N/A	N/A	N/A	80 (2.9)–250 (9.2)	360 (13)–320 (12)	470 (17)–360 (13)	3.5 (1.2)–4.8 (1.7)	NO_3^- = 12–2.0 NH_4^+ = 56–2.7 DON = 18–0.7 PO_4^{3-} = 4.1–0.8
Rivers	70–1700	8.9–7.4	4.0–7.0	31–29	1.0–0.3	620 (230)–13,000 (4600)	280 (100)–12,000 (4300)	2200 (790)–49,000 (18,000)	70 (26)–510 (190)	NO_3^- = 88–98 NH_4^+ = 44–97 DON = 82–99 PO_4^{3-} = 96–99
Total in Mobile Bay	88–1712	N/A	N/A	N/A	N/A	700 (233)–13,250 (4609)	640 (293)–12,320 (4312)	2670 (807)–49,360 (18,013)	73 (27)–515 (190)	100

The table includes values of SGD fluxes at each study site (from Montiel et al. 2018) and river discharge during the dry and wet seasons, nutrient concentrations, nutrient fluxes, and the relative importance of each nutrient to the total nutrients loading of Mobile Bay considering both river- and SGD-derived inputs

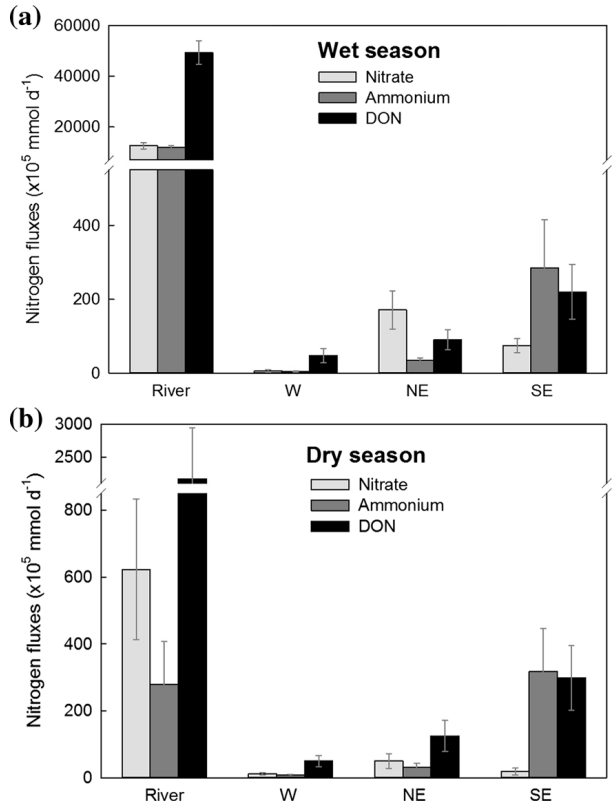

Fig. 6 River-derived and SGD-derived nitrogen fluxes (NO_3^-, NH_4^+, and DON) to Mobile Bay on the western, northeastern, and southeastern shores during the wet (**a**) and dry (**b**) seasons. Most of the SGD-derived nitrogen inputs to Mobile Bay occurred on the southeastern and northeastern shores, representing an average of 93% of the total SGD-N in the bay

Discussion

Evaluating nutrients loading to Mobile Bay

Spatial variability of SGD-derived nutrient fluxes

During this study, we found that the SGD-N and -P fluxes are delivered preferentially to the east shore of Mobile Bay. This uneven nutrient flux distribution is, in part, a result of the preferential SGD pathways in the local coastal aquifer (Montiel et al. 2018). We found that more than 90% of the total SGD-derived N inputs to the bay occurred on the east shore, with two-thirds occurring on the southeastern shore and one-third on the northeastern shore. In contrast, less than 10% of the total SGD-N were delivered to the western shore (Table 3). Additionally to this uneven spatial distribution of the N fluxes across the bay, we found significant differences in the distribution of the N speciation (NO_3^-, NH_4^+, and DON) between the study sites (Fig. 6). During this study, half of the total N delivered via SGD to Mobile Bay was in the form of DON and more than one-third as NH_4^+, while NO_3^- only accounted for less than 20% of the total SGD-N inputs (Fig. 6).

We also found that the southeastern section (study site TS-SE) receives close to 90% of all the SGD-derived NH_4^+, and two-thirds of the DON (Table 3). Indeed, during this three-year study groundwater at study site TS-SE was always anoxic with an average DO concentration of 0.8 mg L^{-1} (Fig. 5). These highly anoxic conditions were reflected in the receiving shallow surface waters of the bay which had an average DO of 2.7 mg L^{-1} (Fig. 1 in Online Appendix). Under these conditions, the NO_3^- fluxes to the east shore accounted for only one-third of the total SGD-derived NO_3^- flux to Mobile Bay (Table 3).

The N speciation on the northeastern shore of the bay (study site TS-NE), showed the opposite pattern. We found that two-thirds of all SGD-derived NO_3^- fluxes in the bay occurs in this section, but only 10% of the NH_4^+, and one-fifth of the SGD-derived DON fluxes (Fig. 6; Table 3). This N speciation and spatial distribution are consistent with the higher groundwater DO measured at this site, which was on average 3.9 ± 1.0 mg L^{-1}. We suggest that the observed oxic conditions on the northeastern shore are most likely resultant of higher infiltration rates through the shallow coarse sand layer with a much higher hydraulic conductivity (58 m day^{-1}) compared to the other study sites (Fig. 2c). However, these conditions reflect only the top layer of the surficial aquifer at the beach face. The coarse sand layer that we recovered in the deep core was artificially added during the development of the area in the 70s. Thus, although it impacts SGD and nutrient fluxes, it does not represent the natural shallow marine sediment environment of the east shore of Mobile Bay. Based on shallow geophysics surveys (electrical resistivity tomography or ERT and continuous resistivity profiling or CRP the peat layer is also present at this study site underlaying the coarse sand layer along the northeastern shore of Mobile Bay (Fig. 2c) (Montiel et al. 2018). We have evidence that the groundwater plume percolates partially through the peat layer along $\sim$ 80 m from the shore (Fig. 2c) (Montiel et al. 2018). However, our shallow intertidal piezometers at this study site did not capture the slightly deeper peat

layer and therefore, the nutrient fluxes measured on the northeastern shore during this study should be considered as conservative estimates.

In comparison, we found that the western shore (study site TS-W) of Mobile Bay receives negligible ($\sim$ 1% of the total) nitrogen via SGD compared to the total bay loading (Fig. 6; Table 3). In this section more than 60% of the SGD-N occurred in the form of DON, while NH_4^+ and NO_3^- represented one quarter and about 15%, respectively. As discussed in Montiel et al. (2018), SGD in this section is impeded by a silt layer, whose presence was confirmed both by ERT measurements and multiple sediment cores collected in the northern and southern ends of its shoreline.

During this study the SGD-derived PO_4^{3-} fluxes to Mobile Bay were one order of magnitude lower than the N-fluxes. These findings are consistent with other studies in a variety of coastal environments (e.g. Lee et al. 2009; Santos et al. 2009; Rodellas et al. 2014). However, the spatial distribution of SGD-derived PO_4^{3-} inputs to Mobile Bay were also partially controlled by the SGD fluxes and were thus similar to the N-fluxes pattern. More than 90% of the total PO_4^{3-} flux in the bay occurred on the east shore, where two thirds were delivered to the southeastern shore and the rest to the northeastern shore (Table 3).

Temporal variability of nutrient fluxes

The total SGD-derived nutrient inputs to Mobile Bay were constant throughout the year with a seasonal variability of less than 5% for N and less than 30% for PO_4^{3-} when comparing the dry and wet seasons (Table 3). This even temporal distribution was result of the combination of a significantly higher nutrient concentration in groundwater during the dry season (Fig. 5) and the relatively lower SGD rates during that season (Montiel et al. 2018). However, we observed important site-specific temporal variations for each nutrient (Table 3). Particularly, on the east shore (at study sites TS-SE and TS-NE) the SGD-NO_3 fluxes increased by 75% during the wet season. We also observed more than 30% SGD-DON decrease during the wet season compared to the dry season (Table 3). In comparison, the SGD-derived PO_4^{3-} fluxes showed a different behavior in all study sites. On both the northeastern and the western shores, SGD-PO_4^{3-} was about 70% and 50% lower during the wet season respectively, whereas on the southeastern shore we observed a two-third decrease. In contrast, the river-derived N fluxes during the dry and wet seasons varied by more than an order of magnitude due to the large seasonal fluvial discharge fluctuations as the concentrations in river water remained fairly constant (Fig. 7). Similarly, the river-derived PO_4^{3-} fluxes were more than seven times higher during the wet season (Fig. 7).

When comparing the total SGD-derived and river-derived nutrient fluxes to Mobile Bay during the wet season (see "Nutrient fluxes via SGD and river discharge" section), we found that SGD represented only a small portion (less than 3%) of the nutrient (NO_3^-, NH_4^+, DON, and PO_4^{3-}) loadings of the bay (Fig. 7a). However, during the dry season when the river discharge is considerably lower, we found that SGD accounted for $>$ 10% of the NO_3^-, $>$ 50% of the NH_4^+, $>$ 15% of the DON, and about 5% of the

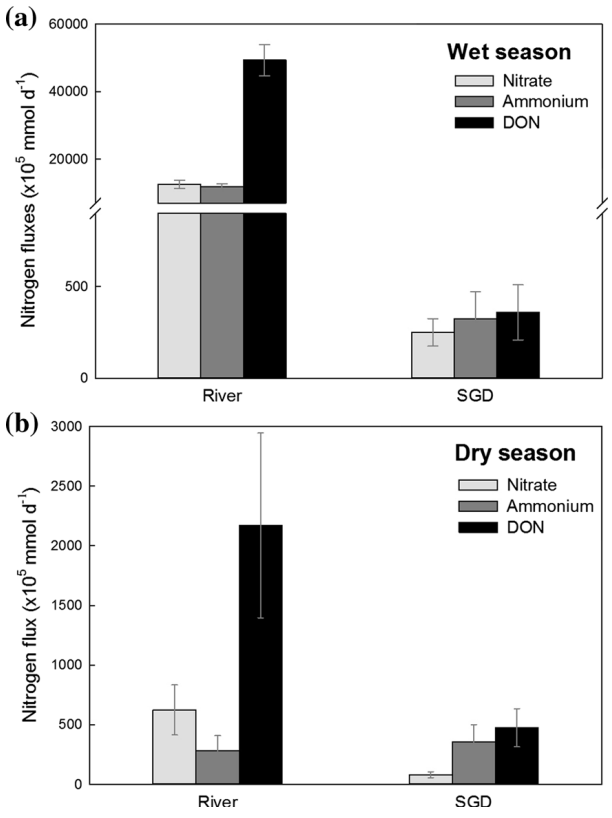

Fig. 7 River-derived and total SGD-derived nitrogen fluxes (NO_3^-, NH_4^+, and DON) to Mobile Bay from all sections during the wet (**a**) and dry (**b**) seasons. NH_4^+ and DON were the main forms of nitrogen delivered to Mobile Bay via SGD during bot the dry and wet seasons, being relatively more important to the total nitrogen loading of Mobile Bay during the dry season (56% and 18% of the total respectively)

PO_4^{3-} budgets (Fig. 7b). Considering the total inorganic and organic N inputs to the bay, SGD accounted for more than 20% of the total N inputs to Mobile Bay during the dry season (Table 3). The relatively constant inputs of nutrients via SGD in Mobile Bay throughout the year compared to the highly fluctuating river discharge determined the significantly higher importance of SGD in Mobile Bay during the dry season.

To compare the SGD-derived nutrients fluxes in Mobile Bay to other estuaries worldwide, we normalized the fluxes by the SGD seepage area (assessed in Montiel et al. 2018) and extrapolated the daily SGD-derived nutrient fluxes to annual nutrient loading to the bay. We calculated that in Mobile Bay SGD provided 15 mol m^{-2} $year^{-1}$ (34×10^6 mol $year^{-1}$) of N and 0.1 mol m^{-2} $year^{-1}$ (0.2×10^6 mol $year^{-1}$) of PO_4^{3-} to the annual nutrients budget (Table 3). For comparison, when normalized by the seepage area Charette et al. (2001) found that the total N delivered by SGD to the Waquoit Bay estuary (Massachusetts, USA) was 0.2 mol m^{-2} $year^{-1}$ (0.8×10^6 mol $year^{-1}$), which is almost two orders of magnitude lower compared to Mobile Bay (15 mol m^{-2} $year^{-1}$) (Table 3). Similarly, in Tampa Bay (Florida, USA) Kroeger et al. (2007) found a total N specific flux of 4.7 mol m^{-2} $year^{-1}$ (6.9×10^6 mol $year^{-1}$) via SGD, also significantly lower than Mobile Bay (15 mol m^{-2} $year^{-1}$). The shallow sediments of both Waquoit Bay and Tampa Bay are comprised of sand and gravel with low organic matter content (Charette et al. 2001; Slomp and Van Cappellen 2004; Kroeger et al. 2007). In contrast, in the Neuse River Estuary (North Carolina, USA) Null et al. (2011) showed that NH_4^+ was also the dominant form of nitrogen in SGD, providing alone about the same nitrogen inputs (15 mol m^{-2} $year^{-1}$) as in Mobile Bay (Table 4). The authors attributed the high NH_4^+ fluxes via SGD to slow groundwater flow and high organic matter degradation in the coastal sediments, evidencing the importance of the shallow hydrogeologic characteristics in estuaries (Null et al. 2011; Spiteri et al. 2008).

Conceptual model of SGD-delivered N and P fluxes to Mobile Bay

To better understand the sources and transformations of N- and P-nutrients in groundwater from the coastal aquifer along the Mobile Bay shoreline, we

Table 4 Groundwater specific nutrient fluxes from the inland zone of the Miocene–Pliocene Aquifer to the intertidal zone of the aquifer, fluxes from the intertidal zone to Mobile Bay as SGD, and net fluxes after groundwater flows through the intertidal zone

	Nutrient	Inland zone of the Miocene–Pliocene Aquifer					Intertidal zone of the Miocene–Pliocene Aquifer (SGD)				Net flux	
		Dry Average concentration (mmol m^{-3})	Wet Average concentration (mmol m^{-3})	Dry Groundwater flow velocity (m day^{-1})	Wet Groundwater flow velocity (m day^{-1})	Dry Specific nutrient flux mmol m^{-2} day^{-1} (mmol m^{-2} $year^{-1}$)	Wet Specific nutrient flux mmol m^{-2} day^{-1} (mmol m^{-2} $year^{-1}$)	Dry Average concentration (mmol m^{-3})	Wet Average concentration (mmol m^{-3})	Dry Groundwater flow velocity (m day^{-1})	Wet Groundwater flow velocity (m day^{-1})	Dry Specific nutrient flux mmol m^{-2} day^{-1} (mmol m^{-2} $year^{-1}$)	Wet Specific nutrient flux mmol m^{-2} day^{-1} (mmol m^{-2} $year^{-1}$)
East shore	NO_3^-	110	110	0.02	0.18	2.2 (790)	20 (7200)	8.0	20	0.17	0.23	1.4 (500)	4.5 (1600)	− 0.8 (− 300)	− 15 (− 5600)
	NH_4^+	7.5	1.1	0.02	0.18	0.2 (55)	0.2 (72)	140	75	0.17	0.23	24 (8600)	17 (6300)	23 (8500)	17 (6200)
	DON	110	50	0.02	0.18	2.2 (800)	9.0 (3300)	130	58	0.17	0.23	22 (8100)	13 (4900)	20 (7300)	4.3 (1600)
	PO_4^{3-}	0.2	0.1	0.02	0.18	0.004 (1.1)	0.01 (1.3)	0.5	0.9	0.17	0.23	0.1 (31)	0.2 (76)	0.08 (30)	0.2 (72)
West shore	NO_3^-	64	120	0.02	0.10	1.3 (470)	12 (4400)	6.7	2.4	0.05	0.06	0.3 (120)	0.2 (55)	− 0.9 (− 340)	− 12 (− 4300)
	NH_4^+	2.6	1.0	0.02	0.10	0.1 (19)	0.1 (32)	4.5	2.2	0.05	0.06	0.2 (84)	0.1 (46)	0.2 (65)	0.02 (9.2)
	DON	16	6.0	0.02	0.10	0.3 (120)	0.6 (220)	28	20	0.05	0.06	1.4 (520)	1.3 (460)	1.1 (400)	0.7 (240)
	PO_4^{3-}	0.1	0.1	0.02	0.10	0.003 (1.0)	0.01 (2.6)	0.2	0.1	0.05	0.06	0.01 (3.7)	0.01 (2.3)	0.01 (2.7)	− 0.001 (− 0.3)

Values of groundwater nutrient concentrations, groundwater flow velocity at each study site during the dry and wet seasons are also included in this table

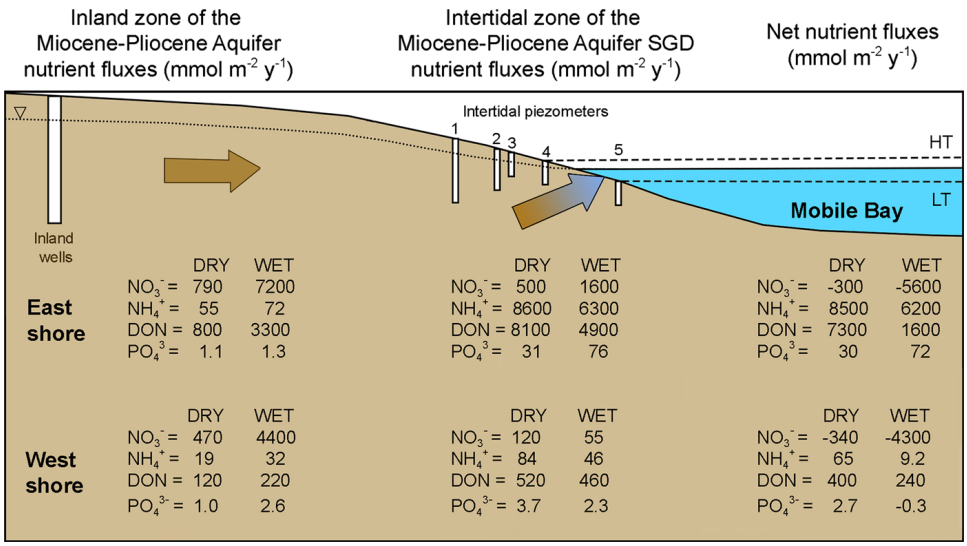

Fig. 8 Schematic profile showing the annual groundwater specific nutrient fluxes from the inland zone of the Miocene–Pliocene Aquifer to the intertidal zone of the aquifer, fluxes from the intertidal zone to Mobile Bay as SGD, and net fluxes after groundwater flows through the coastal sediments. The coastal sediments at the intertidal zone generated negative net fluxes of NO_3^- and positive net fluxes of NH_4^+, DON, and PO_4^{3-}. The sketch is not drawn to scale vertically or horizontally for an easier comparison

constructed a conceptual model that illustrates the N and P specific fluxes on the east and west shores from inland to the intertidal zone and to Mobile Bay (Fig. 8). For each shore, the boundaries of these box-models were defined by the distances between the farthest inland groundwater wells sampled during this study, and the nests of intertidal piezometers (Pz-1 to -5) installed at the SGD zone during this study (Figs. 1, 8). For reference, on the east shore this distance is 3.1 km, and it is 1.7 km on the west shore (Fig. 1). Based on evaluations conducted by Gillett et al. (2000), Dowling et al. (2004), and Ellis et al. (2013) the groundwater flow velocities in the inland part of the Miocene–Pliocene coastal aquifer are between 0.02 and 0.18 m day^{-1} on the east shore, and between 0.02 and 0.10 m day^{-1} on the west shore (Table 4). To calculate site- and season- specific nutrient fluxes between the inland wells and the intertidal piezometers, we used nutrient concentrations obtained during this study recovered from the inland wells. To calculate the SGD-nutrient fluxes delivered to Mobile Bay in the intertidal zone of the Miocene–Pliocene Aquifer, we used seepage velocities reported in Montiel et al. (2018), which are also site- and season-specific based on radiotracers mass balance models and seepage meters measurements, and nutrient concentrations reported in this study. In all scenarios, specific nutrient fluxes (in mmol m^{-2} day^{-1}) were calculated by multiplying average nutrient concentrations (mmol m^{-3}) in groundwater collected during wet or dry seasons by the groundwater flow velocities (m day^{-1}) assessed for each season.

Applying this conceptual model and boundary conditions on the east shore we found that the annual groundwater N-flux in the inland zone of the Miocene–Pliocene Aquifer was on average 6100 mmol m^{-2} $year^{-1}$. This flux was mainly distributed between NO_3^- (4000 mmol m^{-2} $year^{-1}$) and DON (2000 mmol m^{-2} $year^{-1}$) with large seasonal variations, where both fluxes were one order of magnitude higher during the wet season compared to the dry season. On the other hand, the annual NH_4^+ flux in this area was two orders of magnitude lower (64 mmol m^{-2} $year^{-1}$) and did not vary throughout the year (Table 4; Fig. 8). On the east shore of Mobile Bay, the shallow Miocene–Pliocene Aquifer in the inland zone consists of quarzitic sand deposits with low to almost absent organic matter content and a hydraulic conductivity of 10–20 m day^{-1} (Fig. 1) (Chandler et al. 1985; Gillett et al. 2000; Dowling et al. 2004). Based on previous studies conducted by Murgulet and Tick (2009, 2013) NO_3^- was the main form of N in this area reaching groundwater concentrations as high as 1600 mmol m^{-3}. Although we did not find such high levels of NO_3^- in the same wells,

average NO_3^- concentrations in the inland wells (SE-Well-1 and -2), installed at a depth of 10–12 m, were always much higher (110 mmol m^{-3}) compared to concentrations in groundwater recovered from the intertidal piezometers (14 mmol m^{-3}) (Table 4). For comparison, NH_4^+ (3 mmol m^{-3}) and DON (80 mmol m^{-3}) were relatively lower, while the average annual DO was 5.6 mg L^{-1}. We attribute this high NO_3^- to the agricultural activities present in this zone that represent two-thirds of the total land use (Fig. 1). The main agricultural crops in this part of southern Alabama are cotton and corn, which receive rigorous fertilization twice a year, once in the spring (March–April) and once in the fall (October) using both inorganic and organic fertilizers (https://www.nass.usda.gov/Surveys). On the other hand, the average annual P flux in the inland zone was much lower (1.2 mmol m^{-2} $year^{-1}$) compared to the N fluxes and showed no seasonal variability (Fig. 8). We suggest that these low P fluxes result from the observed oxic conditions under which PO_4^{3-} is removed through sorption onto minerals and co-precipitation (Robertson 1995; Weiskel and Howes 1992; Zanini et al. 1998).

When applying the same mass-balance flux approach to the intertidal zone of the east shore of Mobile Bay (Fig. 8), we found that the average annual N-flux delivered by SGD to Mobile Bay was about 15,000 mmol m^{-2} $year^{-1}$, producing a net total N surplus of about 8800 mmol m^{-2} $year^{-1}$. However, unlike the inland zone, the largest portion of the N-fluxes in the intertidal zone of the Miocene–Pliocene Aquifer occurred in equal portions as NH_4^+ (7400 mmol m^{-2} $year^{-1}$) and DON (6500 mmol m^{-2} $year^{-1}$) with a smaller seasonal variability (Fig. 8). In contrast, the average annual NO_3^- fluxes in the intertidal zone were only 1100 mmol m^{-2} $year^{-1}$, resulting in a net negative balance of about − 2900 mmol m^{-2} $year^{-1}$. These SGD-NO_3^- fluxes showed the largest seasonal variability of all nutrients with an annual flux three times larger during the wet season (Fig. 8). Although still lower than SGD-delivered N loadings, the average net P flux to Mobile Bay via SGD was more than one order of magnitude higher (54 mmol m^{-2} $year^{-1}$) compared to the inland zone (1.2 mmol m^{-2} $year^{-1}$). We suggest that this can be caused by an enhanced PO_4^{3-} solubility under anoxic conditions via desorption as groundwater flows through the coastal sediments (Figs. 2b, 5) (Weiskel and Howes 1992; Slomp and Van Cappellen 2004).

Using the conceptual model in the inland zone of the west shore of Mobile Bay, we found significantly lower nutrient fluxes compared to the east shore with an annual average total N flux of 2600 mmol m^{-2} $year^{-1}$ and a P flux of about 1.8 mmol m^{-2} $year^{-1}$ (Table 4). We observed a particularly pronounced seasonal pattern in the NO_3^- fluxes with an order of magnitude higher flux during the wet season (Fig. 8). Since this area is relatively pristine, i.e. two-thirds is dominated by forests and wetlands, we attribute the higher N fluxes to the seasonal variability of groundwater flow velocity. Interestingly, the annual SGD-delivered total N fluxes in the intertidal zone of the Miocene–Pliocene Aquifer were four times lower (640 mmol m^{-2} $year^{-1}$) compared to the inland fluxes, with no significant seasonal variability (Fig. 8). Furthermore, when we calculate the net fluxes between the two zones (i.e. inland minus nearshore), we found large total N loss of about − 4000 mmol m^{-2} $year^{-1}$. When looking at the distribution of the individual N-speciation, it was apparent that the NO_3^- net loss of − 2300 mmol m^{-2} $year^{-1}$ contributed the most to the N deficit observed in the transition from the inland zone to the intertidal zone. For comparison, although the average net P flux was one order of magnitude lower (1.2 mmol m^{-2} $year^{-1}$) compared to the N fluxes, we detected a net surplus of PO_4^{3-} in the transition between inland and the intertidal zone as well as an important seasonal variability (Fig. 8).

Based on the calculated annual groundwater fluxes in the coastal Miocene–Pliocene Aquifer, we conclude that the intertidal coastal sediments on both shores of Mobile Bay serve as a sink for the high NO_3^- loading observed in the inland groundwater, transforming NO_3^- into NH_4^+ and DON. However, we found that concurrently to this N transformation resulting in overall net loss of NO_3^-, there is a significant net production of total N as NH_4^+ and DON (8800 mmol m^{-2} $year^{-1}$) on the east shore, resulting in a significant positive N export via SGD of 15,000 mmol m^{-2} $year^{-1}$ to the bay. These large N fluxes were accompanied by a net production of about 51 mmol m^{-2} $year^{-1}$ of PO_4^{3-} on the east shore of Mobile Bay. Because the inland section of the aquifer is mostly quartz with very low organic content, we hypothesize that the net production of N and P

observed on the east shore of Mobile Bay is generated by the peat layer that is only present on this shore, explaining the large spatial differences in SGD-N and -P fluxes observed between shores.

Microbial-mediated transformations of nutrients in groundwater

To be able to identify the biogeochemical transformations responsible for the observed nutrient transformations in the Miocene–Pliocene Aquifer, we used the microbial community composition as a proxy for dominant metabolic pathways in groundwater. Metabolic interpretations were collaborated with site-specific redox conditions and rate of anthropogenic/natural nutrients supply.

As we suggested earlier, the high levels of NO_3^- and DON (Table 2) detected in the inland wells of the east shore are, in part, a result of the abundant agricultural activities in this area. However, oxic conditions (Table 2) and presence of genera *Vogesella*, *Sphingomonas*, and *Acinetobacter* (Table 2 in Online Appendix) also indicate that the high DON observed in this inland zone (Table 2) may undergo aerobic mineralization. The final degradation products of this mineralization result in nitrite (NO_2^-) which is then fully oxidized to NO_3^- via nitrification as confirmed by the high relative proportion of nitrifier genus *Nitrospira* (Table 2 in Online Appendix) (Watson et al. 1986; Weiss et al. 2007).

At the intertidal zone of the southeastern shore, the shallow groundwater collected from a depth of up to 60 cm using a multi-level piezometer SE-Pz-4.5 (samples SE-Pz-4.5-A and -B) (Figs. 2a, 3), showed mostly aerobic microbial communities (Table 2 in Online Appendix). The high sequence proportions of *Cyanobiaceae*, oxygen-producing autotrophic bacteria, and strictly aerobic bacteria such as *Deinococcus* and *Aquicella* indicate that the upper-most sand layer is a well-oxygenated environment (Stanier et al. 1971; Brooks and Murray 1981; Santos et al. 2003; Sangwan et al. 2004). However, at greater depths of 60–150 cm (samples SE-Pz-1, -4.5-C and -4.5-D) using the same piezometer and coinciding with the presence of the peat layer (Fig. 2a), the water was anoxic and dominated by anaerobic microorganisms (Table 2 in Online Appendix). We identified a microbial community of hydrolyzers and fermenters (*Dehalococcoidia*, *Anaerolineaceae*), denitrifiers (*Thermodesulfovibrionia*), iron reducers (*Geobacter*), sulfate-reducing bacteria (*Desulfobacca* and *Desulfatiglans*), and methanogens (*Methanoregula* and *Methanolinea*) commonly found together in highly reducing environment as a syntrophic microbial consortium (Yamada et al. 2006; Kuever 2014a, b; Biderre-Petit et al. 2016; Sun et al. 2016; Liu et al. 2018; Maus et al. 2018). In this peat layer (as in similar organic-rich environments) the hydrolyzers and fermenters initiate the abundant organic matter mineralization, further utilized by nitrate, iron, and sulfate-reducing bacteria; and under lower availability of preferred electron acceptor, by methanogens to produce methane (Hattori 2008).

Some of the identified microorganisms in the peat layer most likely use different electron acceptors depending on the environmental conditions such as tidal variations and seasonal changes in the SGD rate. For instance, some genera from class *Thermodesulfovibrionia* and genus *Geobacter* are known to utilize NO_3^-, Fe^{2+}, and SO_4^{2-} as electron acceptors simultaneously (Lovley et al. 1993; Sekiguchi et al. 2008). As no obligate Fe^{2+} reducing bacteria were found in the peat layer during this study, the N transformations in this sediment layer are most likely dominated by the organic matter mineralization, SO_4^{2-} reduction, and methanogenesis. The thriving community of SO_4^{2-} reducing bacteria can result in significant sulfide (S^{2-}) production, inhibiting the production of NO_3^- via nitrification as observed in "Conceptual model of SGD-delivered N and P fluxes to Mobile Bay" section. However, the production of S^{2-} also lowers the rate of denitrification (An and Gardner 2002). Consequently, the massive net production of NH_4^+ shown in "Conceptual model of SGD-delivered N and P fluxes to Mobile Bay" section must be generated not only by the abundant organic matter mineralization, but also via dissimilatory nitrate reduction to ammonium (DNRA). Sulfate$^-$reducing bacteria are known to have the secondary capacity to implement DNRA because the sulfite reductase is very similar and work constitutively with the nitrite reductase gene NrfA (Widdel and Pfennig 1982; Mitchell et al. 1986; Seitz and Cypionka 1986; Tiedje 1988; Moura et al. 1997). Furthermore, the occurrence of DNRA in the presence of high S^{2-} concentrations has also been reported in coastal sediments of other estuaries and coastal lagoons worldwide (e.g. Rysgaard et al. 1996; An and Gardner 2002; Gardner et al. 2006; Bernard et al. 2015).

Below the peat layer in the transition sand at a depth of 150–180 cm (Fig. 2a), the microbial community in sample SE-Pz-4.5-F was almost entirely comprised of aerobic bacteria (e.g. *Pirelullaceae*, *Gaiellales*, *Nocardioides*, *Mesorizhobium*, *Verrumicrobium*, and *Curvibacter*) (Prauser 1976; Jarvis et al. 1997; Ding and Yokota 2004; Mohamed et al. 2010; Albuquerque et al. 2011). This depth corresponds with the well-oxygenated groundwater flowing from the inland zone of the Miocene–Pliocene Aquifer (Fig. 2b), further supporting that the observed net production of DON and NH_4^+ is naturally originated in the peat layer as SGD occurs to the bay (Fig. 8).

In contrast, in the intertidal piezometers of the northeastern shore (samples NE-Pz-1-A, -B, and EN-Pz-5) installed in the artificial beach coarse sand, we observed the coexistence of obligate aerobic and anaerobic facultative bacteria, indicative of a well-oxygenated environment. We found high sequence proportion of aerobic methanotrophic bacteria (*Methylobacter* and *Methylococcus*) that are also capable of performing nitrification as their key enzyme (methane monooxygenase) is evolutionarily linked with the primary enzyme to oxidize ammonia (ammonia monooxygenase) (Holmes et al. 1995). On the northeastern shore, as SGD occurs, groundwater may be forcing the high amounts of NH_4^+ and methane produced in the peat layer to migrate towards the coarse sand and ultimately to the bay (Fig. 2c). *Methylobacter* and *Methylococcus* are most likely responsible for the lower NH_4^+ and higher NO_3^- concentrations in this study site by converting NH_4^+ into NO_3^- via nitrification using methane as substrate (Hanson and Hanson 1996; Nyerges et al. 2010).

Nutrient sources in Mobile Bay

We strongly suggest that the nutrient inputs via SGD to Mobile Bay and thus its ecological effect on the bay are mostly resultant of the natural lithological composition and biogeochemical transformations in the intertidal zone of the Miocene–Pliocene Aquifer. Although abundant agriculture exists in the Mobile Bay coastal area and impacts the groundwater in the inland zone of the Miocene–Pliocene Aquifer near the fields and farms, we did not find evidence of anthropogenic sources of nutrients in the composition of SGD that enters Mobile Bay. However, we found strong evidence from a wide spectrum of approaches to support a statement that the SGD-nutrient fluxes to Mobile Bay have a natural origin.

Lithological evidence

Sediment cores recovered during this study from both the northeastern and southeastern shores of Mobile Bay showed the presence of an organic-rich (up to 36%) peat layer along the east shore. Detailed shallow geophysical exploration (both ERT and CRP surveys) revealed that this layer extends at least 110 m offshore along the east shore of the bay (Montiel et al. 2018). Combined ERT time-series measurements of the subsurface during falling tide and sediment properties analyses of the cores confirmed that the peat layer has relatively high hydraulic conductivity (8.2 m day^{-1}) allowing the occurrence of SGD (Montiel et al. 2018). Furthermore, we found that the peat layer creates anoxic conditions in groundwater at the intertidal zone along the east shore and generates extremely high net fluxes of NH_4^+ and DON (see "Conceptual model of SGD-delivered N and P fluxes to Mobile Bay" section). However, we found that the conditions observed on the east shore are not ubiquitous in Mobile Bay. Parallel geophysical and lithological investigations of the shallow aquifer structure and composition on the west shore did not reveal the same conditions. ERT and CRP surveys as well as multiple core sedimentological characterization showed a spatially uniform fine-grained lithology, which was confirmed to be a silt layer with very low permeability based on the recovered cores (Montiel et al. 2018). In addition, we found that the organic content of the silt layer on the west shore was low (only 11%) and we did not identify the distinct peat layer found on the east shore (Montiel et al. 2018). In turn, although anoxic conditions were present, we found negative net N fluxes through the coastal aquifer on this shore, showing that the coastal sediments on the west serve only as a sink of nutrients. Therefore, we can conclude that the peat layer on the east shore is a natural source of N to Mobile Bay. The important net production of N, only observed on the east shore, indicated that the organic matter mineralization in the peat layer must be responsible for the additional N fluxes as NH_4^+ and DON. Additionally, the net loss of NO_3^- on both the west and east shores of the bay indicate that denitrification and DNRA are occurring in the coastal sediments as described in "Conceptual model of

SGD-delivered N and P fluxes to Mobile Bay" section. Bernard et al. (2015) demonstrated in a coastal lagoon near Mobile Bay (Little Lagoon) that DNRA and denitrification occur during both wet and dry seasons in this area. Furthermore, Bernard et al. (2015) found that during the dry season, when *Jubilees* and HABs occur, DNRA is the dominant NO_3^- reduction pathway. Similarly, Domangue and Mortazavi (2018) found that in the coastal sediments of Weeks Bay, an estuary connected to Mobile Bay on the east shore (Fig. 1), DNRA is also the primary process of nitrate reduction, exceeding denitrification.

Evidence from stable isotopes

To identify the sources of N in Mobile Bay we utilized the $\delta^{15}N_{NO_3}$ and $\delta^{18}O_{NO_3}$ isotopic signatures measured in the two main water end-members entering the bay including groundwater and river water inputs (Amberger and Schmidt 1987; Kendall 1998; Kendall et al. 2007; Xue et al. 2009). Using this approach, we were able to (1) identify possible sources of N and (2) confirm the microbial metabolic pathways and N transformations in the shallow coastal aquifer and Mobile Bay waters.

The $\delta^{15}N_{NO_3}$ and $\delta^{18}O_{NO_3}$ isotopic signatures measured in the study area suggest the influence of three main sources of NO_3^- in the Mobile Bay system including inorganic fertilizers (both NO_3^-- and NH_4^+-based), organic fertilizers (e.g. manure), and organic soil mineralization. Based on our data, the main source of N in Mobile Bay is the mineralization of organic soil N (Fig. 9a). This observation confirms our findings based on nitrogen mass-balances (Fig. 8). The $\delta^{15}N_{NO_3}$ and $\delta^{18}O_{NO_3}$ values measured in both end-members, river water and groundwater, also indicate that the main source of N is the soil N (Fig. 9a; Table 1 in Online Appendix). We found that only groundwater collected from the inland wells showed isotopic values indicating a fertilizers source (Fig. 9a; Table 1 in Online Appendix). The absence of isotopic values indicating anthropogenic sources such as fertilizers, sewage waste and manure at the intertidal zone suggests that the soil N present in the coastal sediments is the main source of N to Mobile Bay (Fig. 9a). Similarly, Beebe and Lowery (2018) also observed on the western shore that the main source of N in groundwater was the soil organic matter

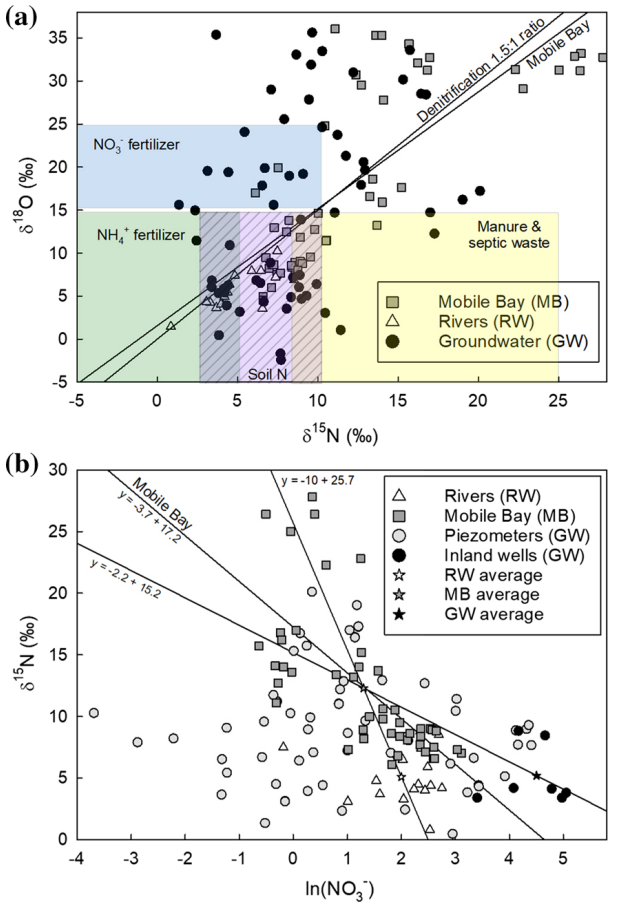

Fig. 9 **a** Cross plot showing the nitrate stable isotopes $\delta^{15}N_{NO_3}$ and $\delta^{18}O_{NO_3}$ values measured in rivers, Mobile Bay, and in groundwater. Samples collected on the western, southeastern, and northeastern shores are represented as white, grey, and black circles, respectively. Theoretical values for anthropogenic (NO_3^- and NH_4^+ fertilizers, manure and septic waste) and natural (organic nitrogen in the sediments or soil) sources of nitrate $\delta^{15}N$ and $\delta^{18}O$ signatures are shown in all panels (Amberger and Schmidt 1987; Kendall 1998; Kendall et al. 2007; Xue et al. 2009). The theoretical denitrification line of $\delta^{18}O$:$\delta^{15}N$ as 1.5:1 is shown in all panels based on Kendall et al. (2007) and Murgulet and Tick (2013). **b** Rayleigh plot comparing $\delta^{15}N_{NO_3}$ values and the natural log of nitrate concentrations of all samples collected during this study. The linear trends of Mobile Bay water samples are indicated in the panel together with linear trends from the inland wells average and rivers average to the Mobile Bay average. Slopes from the two NO_3^- pools (inland wells and rivers) to the Mobile Bay average indicate their kinetic enrichment factor (ε)

mineralization, whereas no evidence of anthropogenic N inputs was found.

We found that significant denitrification and biological uptake occurs both in groundwater and in bay waters. Groundwater values are scattered around the denitrification line (Fig. 9a) suggesting a main trend

but more complex in nature where the $\delta^{15}N_{NO_3}$ and $\delta^{18}O_{NO_3}$ enrichment must be consequence of further fractionation via other biogeochemical processes in addition to denitrification. As described in "Conceptual model of SGD-delivered N and P fluxes to Mobile Bay" nd "Microbial transformations of nutrients in groundwater" sections, DNRA and biological uptake must also contribute to the N transformations in the groundwater before entering the bay. In Mobile Bay waters the fractionation of $\delta^{15}N_{NO_3}$ and $\delta^{18}O_{NO_3}$ also indicate that denitrification is probably responsible for significant removal of N inputs entering the bay from rivers and SGD (Fig. 9a). The maximum isotopic values measured in Bon Secour Bay ($\sim$ 16–27‰) and minimum near the river delta ($\sim$ 5–10‰) indicate that NO_3^- experiences denitrification from the two main routes of entrance in the bay, rivers and SGD on the northeastern shore (Fig. 8a, b) (Kendall et al. 2007).

The isotopic kinetic fractionation derived from denitrification and the intensity of this process can be further determined by an enrichment factor (ε) that can be obtained from a Rayleigh plot comparing $\delta^{15}N_{NO_3}$ and the natural log of nitrate concentrations (Fig. 9b) (e.g. Kendall 1998; Granger et al. 2008; Ryabenko 2013). Based on the Rayleigh trends, in Mobile Bay waters about 50% of the NO_3^- loss is indeed caused by denitrification with a $\delta^{15}N_{NO_3}$ enrichment factor of − 3.7‰, similar to other surface water environments (Fig. 9b) (e.g. Sebilo et al. 2003; Yevenes et al. 2016; Harms et al. 2019). Considering the two original pools of NO_3^- (groundwater and rivers) of Mobile Bay in the Rayleigh plot, the two enrichment factors calculated from their average to the Mobile Bay waters average clarified the dominant biogeochemical processes occurring in the bay (Gruber 2004; Ryabenko 2013). We found that a ε value of − 2.2‰ from the inland wells pool indicates that as NO_3^- percolates through the intertidal sediments to the bay waters via SGD, NO_3^- experiences both benthic denitrification and biological uptake in the shallow sediments (Fig. 9b). The isotopic enrichment of the riverine pool of NO_3^- in the bay, with a ε value of − 10‰, indicates that biological uptake is the main process of N removal and to a lower extent denitrification in the water column (Fig. 9b). The biological uptake of NO_3^- in the bay is also supported by the spatial distributions of NO_3^- concentrations in the bay. Most of the NO_3^- inputs (8–98% of the total NO_3^-) to the bay occurred via riverine discharge and NO_3^- concentrations gradually decreased from the river delta (9–26 mmol m^{-3}) to Bon Secour Bay (0.1–1.2 mmol m^{-3}) (Fig. 2a in Online Appendix).

Nitrification was not observed to occur, at least significantly, in the study area considering that the two routes of N entrance (SGD and rivers) in Mobile Bay have much higher NO_3^- concentrations and depletion of both $\delta^{15}N_{NO_3}$ and $\delta^{18}O_{NO_3}$ compared to bay waters (Gruber 2004; Ryabenko 2013).

Evidence from organic source-composition characterization

We analyzed the DOM composition entering to Mobil Bay via rivers and groundwater to further confirm the hypothesis of a natural origin of N to the system. In Mobile Bay surface water, humic-like degradation components C1 and C2 were detected in almost equal percentage (28% and 34%), whereas protein-like component C3 was 38%. The highest percentages of components C1 and C2 were found near the river delta and the northeastern shore. We suggest that the river discharge and SGD through the peat layer on the east shore are the main sources of components C1 and C2 indicative of decaying plant material (Fig. 5a–c in Online Appendix).

In groundwater collected from the multi-level piezometer (SE-Pz-4.5) on the east shore of Mobile Bay, where the peat layer is located, DOM was primarily composed of humic-like components C2 (43%) and C1 (29%) (Fig. 10a). This is a clear indication that SGD is transporting the degradation products of terrestrial organic matter to Mobile Bay waters. We hypothesize that the presence of components C1 and C2 in the peat layer can result from decomposing salt marsh plants such as *Juncus roemerianus*, *Spartina alterniflora* and freshwater marsh *Typha* and *Schoenoplectus* (undifferentiated) common in the Mobile Bay area (Cory and McKnight 2005; Fellman et al. 2010; Lu et al. 2015; Smith and Osterman 2014; Wheeler et al. 2017). To confirm the origin of the peat layer on the east shore of Mobile Bay and the origin of the degradation products released by SGD, we also conducted stable isotope analyzes of the organic matter present in sediment core TS-SE recovered at study site TS-SE on the southeastern

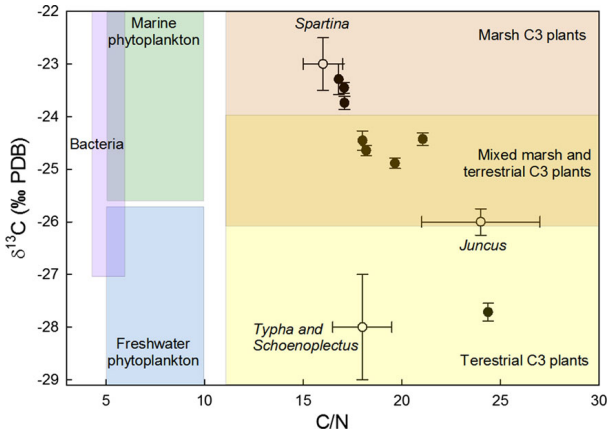

Fig. 10 Cross plot showing the relationship between $\delta^{13}C_{org}$ and C/N of the of the organic matter present in the peat layer (B) from sediment core TS-SE. Ranges of all possible theoretical origins of organic matter (bacteria, marine and freshwater phytoplankton, marsh and terrestrial C3 plants) are represented as defined by Lamb et al. (2006) and Guerra et al. (2015). Three specific regional end-member values measured in Mobile Bay are also shown for marsh plant species *Spartina alterniflora* (*Spartina*), *Typha* and *Schoenoplectus* undifferentiated (*Typha* and *Schoenoplectus*), and *Juncus roemarianus* (*Juncus*) as presented by Smith and Osterman (2014). These data highlight the importance of terrestrial organic matter to Mobile Bay. All samples fall in the marsh and terrestrial C3 plants value range and regional *Spartina alterniflora* and *Juncus roemarianus* end-members

shore (Fig. 3). The average C/N atomic ratios of 19 of this layer (Fig. 4; Table 1) are similar to other peat sediments (fine-grained organic-rich) sediments identified elsewhere (e.g. Stanek and Silc 1977; Schnurrenberger et al. 2003; Lambert et al. 2008). When comparing the C/N ratios with the $\delta^{13}C_{org}$ isotopic composition along the core profile, and using reference values reported by Meyers (1997) and Lamb et al. (2006), we identified two organic matter sources: (1) terrestrial C3 plants litter (e.g. pine and oak tree debris) and (2) remains of C3 plants of marsh environment (Fig. 10). The C/N values of all samples, except for the shallowest sample (45 cm), are closely clustered in the range between 17 and 21 with a narrow $\delta^{13}C_{org}$ isotopic signatures of 23–28‰ (Fig. 10), confirming that marsh C3 plants are the main source of organic matter in the peat layer (Guerra et al. 2015). Furthermore, based on the Mobile Bay end-members as presented by Smith and Osterman (2014), the plant remains conforming the peat layer most likely correspond to marsh species *S. alterniflora* and *J. roemarianus* (Fig. 10).

Ecological implications of SGD

We hypothesize that the occurrence of SGD-derived nutrient fluxes focused on the east shore of Mobile Bay, must have significant effects on the nutrient balance and the ecological health of the bay.

Loesch (1960) indicated that *Jubilee* events are linked to water hypoxia and water column stratification during the summer months (dry season). Montiel et al. (2018) further demonstrated that the groundwater anoxia produced by the peat layer as SGD occurs on the east shore is directly correlated with the oxygen depletion of the adjacent surface waters but had no evidence of the geochemical transformations that caused the near-bottom water hypoxia. May (1973) showed that *Jubilees* are triggered by a combination of tidal and wind conditions; while Turner et al. (1987) and Park et al. (2007) suggested that the benthic oxygen demand may cause the hypoxia and consequent *Jubilee* events. The spatial distribution of the significant SGD-derived NH_4^+ and DON inputs observed during this study on the east shore coincide exactly with the locations impacted by *Jubilees* (Loesch 1960; May 1973; Montiel et al. 2018). The delivery of anoxic groundwater and reduced forms of N to the water column by SGD through the peat layer may increase the chemical oxygen demand, enhancing hypoxia in the deeper water layer and potentially promoting *Jubilee* events in Mobile Bay. A bottom-up mechanism of hypoxia has been reported in other coastal areas. For instance, Peterson et al. (2016) showed that inputs of anoxic groundwater via SGD were responsible for a significant DO deficit in the water column, leading to hypoxic events in coastal waters of Long Bay, SC. Furthermore, at a larger time scale, the delivery of DOM and NH_4^+ via SGD can also promote eutrophication and even more severe DO depletion (D'Avanzo and Kremer 1994; Paerl 1997; Paerl 1998; Diaz and Rosenberg 2008; Howarth et al. 2011; Null et al. 2011). Often, this bottom-up generated hypoxia is then maintained by the physical and climatic conditions during these events leading to stratification (e.g. McCoy et al. 2011).

A strong evidence supporting this hypothesis is the absence of *Jubilees* on the western shore of Mobile Bay. May (1973) showed that hypoxia also occurred along the western shore when an extensive *Jubilee*

only took place on the eastern shore, triggered by the easterly winds. During the summer months slight southwest to westerly winds are common in Mobile Bay; however, *Jubilees* have never occurred on the western shore. As discussed in Loesch (1960), the lack of topographic protection against winds near the shore may restrict the occurrence of *Jubilees* on the western shore. Nevertheless, it is likely that the absence of the peat layer combined with the insignificant SGD inputs found on the western shore, could be limiting the occurrence of *Jubilees* in this area. Furthermore, SGD-derived nutrient inputs on the western shore always represented $< 2\%$ of the total inputs in Mobile Bay for all nutrients, restricting the potential effect of SGD on *Jubilees*. Additional evidence strongly indicates that *Jubilees* are caused by natural processes and that these events may be affected by SGD-derived nutrient inputs and the presence of a peat layer on the east shore. The historical frequency and intensity of *Jubilees* in Mobile Bay have not varied since at least 1867 although the area has experienced significant development since the 1960s (Loesch 1960; May 1973; Turner et al. 1987; Park et al. 2007). We suggest that because *Jubilees* have been documented to occur historically (> 150 years) in the same locations it is likely that inputs of groundwater and the natural shallow lithology of these areas might be important factors for hypoxia events in Mobile Bay. Rodriguez et al. (2008) examined the formation history of the bay and concluded that Mobile Bay is a flooded estuary formed during the las sea-level transgression about 8000 years ago. During this transgression, large nearshore marsh areas of the bay were flooded and converted into central-basin areas. The lithologic, DOM, sand table isotopes evidences found during this study strongly suggest that the peat layer found in Mobile Bay is composed of vascular plant remnants from the ancient nearshore marsh areas identified by Rodriguez et al. (2008). We suggest that SGD occurring through this decomposing peat layer has historically served as a natural source of significant nutrients and anoxic groundwater on the east shore, contributing to the hypoxia and *Jubilee* events.

The nutrient inputs derived from SGD in Mobile Bay can have further ecological implications in the norther GOM. During the summer, the Mississippi Bight region, to the east of the Mississippi River Delta, experiences extensive and persistent hypoxia (Rabalais et al. 2002). Dzwonkowski et al. (2018) showed that freshwater inputs from Mobile Bay represent the largest contribution to the stratification and oxygen depletion of the northern GOM. The significant delivery of anoxic groundwater as SGD with abundant NH_4^+ and DON inputs in Mobile Bay observed during this study must thus, also influence the regional biogeochemical processes and oxygen budget of the northern GOM.

Although HABs have never been studied in the northern half of the bay, we hypothesize that the SGD-derived nutrient inputs evaluated in this study could also be affecting HABs. N/P ratios in SGD are significantly different from the receiving coastal waters, and thus could potentially result in the ecological disequilibrium that directly affects phytoplankton growth (Kim and Swarzenski 2010). The optimum nutrient uptake by primary producers in typical marine environments occurs at the N/P Redfield ratio of 16:1 during cellular growth (Redfield 1934). As a result, coastal waters where degradation of this planktonic material occurs would follow relatively closely this N/P ratio. However, SGD-delivered excess nitrogen (i.e. high N/P ratios) to the coastal areas often triggers HABs among other ecological impacts (e.g. Yamaguchi et al. 2001; Garcés et al. 2011; Smith and Swarzenski 2012). During this study we found that the average N/P ratio of Mobile Bay waters was exactly 16:1, indication that Mobile Bay is nutrient unlimited. However, the bay's surface waters on the southeastern shore and the southern sector of the western shore showed significant excess of N with N/P values always above 30 and up to 350 (Fig. 11a; Fig. 2e in Online Appendix). Previous studies by Liefer et al. (2009) and Mcintyre et al. (2011) have shown that these two areas are largely impacted by toxic blooms of diatoms. During this study we found that N/P ratio in the Mobile-Tensaw River System was relatively constant and only slightly higher than the Redfield ratio with an average of 21:1 (Fig. 11b). Thus, the excess N observed in the areas impacted by HABs must be affected by the important NH_4^+ inputs delivered by SGD. We found that the N/P ratios measured in groundwater samples in the intertidal zone of the western (79) and southeastern shores (250) were very high (Fig. 11c), coinciding with the areas of highest N/P ratios in Mobile Bay where HABs occur. Previous studies assumed that SGD could affect HABs by delivering the NO_3^- contamination observed in the Miocene-Pliocene Aquifer from nearby agricultural

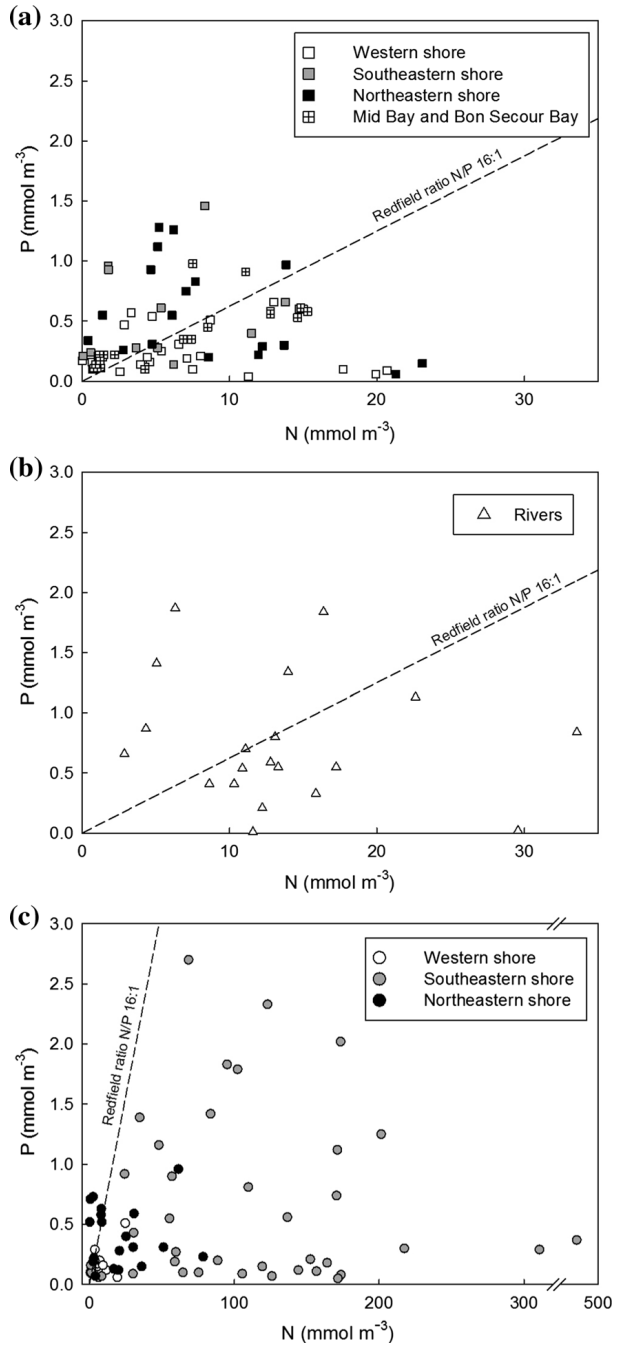

Fig. 11 Cross plot showing the nitrogen (as $NO_3^- + NH_4^+$) and phosphorous (as PO_4^{3-}) concentrations measure in Mobile Bay (**a**), rivers (**b**), and groundwater (**c**). The Redfield molar N/P ratio of 16:1 is shown in all panels for reference. The average N/P ratio in Mobile Bay waters was 16 (Redfield ratio), while in rivers and groundwater the N/P ratios were 21 ± 9 and 270 ± 130, respectively

fertilizers to Mobile Bay (Liefer et al. 2009; Murgulet and Tick 2009; Mcintyre et al. 2011; Liefer et al. 2014). However, we demonstrated here that in the case that HABs are impacted by SGD, the nitrogen inputs are of natural origin produced in the sediments and as NH_4^+ and DON.

Conclusions

Although dominated by river inputs, Mobile Bay receives nearly a quarter of the nutrient loadings via SGD during the dry season, when river discharge is lowest. During the dry season more than 90% of these SGD nutrients fluxes occur on the east shore, coinciding exactly with the time of the year and area where *Jubilees* take place. We found that during the dry season more than half of the total NH_4^+ and 15% of the DON inputs in Mobile Bay are delivered to the east shore via SGD. We hypothesize that the *Jubilee* events are supported by these SGD-derived NH_4^+ and DON inputs during optimum climatic and physical conditions. Additionally, we also hypothesize that the HAB events observed in Mobile Bay can be triggered by the nitrogen excess as NH_4^+ and DON provided by SGD during the summer.

We found that mineralization of the abundant organic matter in a peat layer and DNRA are responsible for the exceptionally high NH_4^+ and DON fluxes delivered by SGD on the east shore of the bay. In contrast to previous studies, we found that the NO_3^- contamination in groundwater from anthropogenic inputs of fertilizers further inland are consumed and transformed by the microbial community in the coastal sediments via denitrification and DNRA. Furthermore, we found that other sources of anthropogenic N and P pollution such as fertilizers, manure and sewage waste are insignificant in Mobile Bay. We demonstrate in this study that these important nitrogen inputs are of natural origin, result of the biogeochemical transformations occurring in the peat layer identified on the east shore of Mobile Bay. We found that this peat layer is comprised of the root system and plant remains of an ancient marsh which history and exact age require further evaluation. We further hypothesize that due to the similar formation history of modern estuaries; natural inputs of nutrients via SGD can also exceed anthropogenic sources in other estuaries worldwide.

Acknowledgements This research was partially funded by the National Science Foundation (NSF OIA-1632825), the 2016

ExxonMobil Summer Fund, the 2015 Gulf Coast Association of Geological Societies Student Research Grant, the University of Alabama Graduate School Research and Travel Support Fund, the UA Department of Geological Sciences W. Gary Hooks and the A. S. Johnson Travel Fund. We also want to thank the Weeks Bay National Estuarine Research Reserve and the Army Corp of Engineers in Mobile for providing technical support during all field campaigns.

References

Adyasari D, Hassenrück C, Oehler T, Sabdaningsih A, Moosdorf N (2019) Microbial community structure associated with submarine groundwater discharge in northern Java (Indonesia). Sci Total Environ 689:590–601

Albuquerque L, França L, Rainey FA, Schumann P, Nobre MF, da Costa MS (2011) *Gaiella occulta* gen. nov., sp. nov., a novel representative of a deep branching phylogenetic lineage within the class Actinobacteria and proposal of Gaiellaceae fam. nov. and Gaiellales ord. nov. Syst Appl Microbiol 34:595–599

Amberger A, Schmidt HL (1987) Natürliche isotopengehalte von Nitrat als Indikatoren für dessen Herkunft. Geochim Cosmochim Acta 51:2699–2705

An S, Gardner WS (2002) Dissimilatory nitrate reduction to ammonium (DNRA) as a nitrogen link, versus denitrification as a sink in a shallow estuary (Laguna Madre/Baffin Bay, Texas). Mar Ecol Prog Ser 237:41–50

Beebe DA, Lowery BA (2018) Seawater recirculation drives groundwater nutrient loading from a developed estuary shoreline with on-site wastewater treatment systems: Mobile Bay, USA. Environ Earth Sci 77:372

Bernard RJ, Mortazavi B, Kleinhuizen AA (2015) Dissimilatory nitrate reduction to ammonium (DNRA) seasonally dominates NO_3^- reduction pathways in an anthropogenically impacted sub-tropical coastal lagoon. Biogeochemistry 125:47–64

Biderre-Petit C, Dugat-Bony E, Mege M, Parisot N, Adrian L, Moné A, Denonfoux J, Peyretaillade E, Debroas D, Boucher D, Peyret P (2016) Distribution of Dehalococcoidia in the anaerobic deep water of a remote meromictic crater lake and detection of Dehalococcoidia-derived reductive dehalogenase homologous genes. PLoS ONE 11:e0145558

Brooks B, Murray R (1981) Nomenclature for "Micrococcus radiodurans" and other radiation-resistant cocci: Deinococcaceae fam. nov. and *Deinococcus* gen. nov., including five species. Int J Syst Evol Microbiol 31:353–360

Burnett WC, Santos IR, Weinstein Y, Swarzenski PW, Herut B (2007) Remaining uncertainties in the use of Rn-222 as a quantitative tracer of submarine groundwater discharge. In: Sanford W, Langevin C, Polemio M, Povinec P (eds) A new focus on groundwater–seawater interactions. IAHS Publication 312, pp 109–118

Callahan BJ, McMurdie PJ, Rosen MJ, Han AW, Johnson AJA, Holmes SP (2016) DADA2: high-resolution sample inference from Illumina amplicon data. Nat Methods 13:581

Cerdà-Domènech M, Rodellas V, Folch A, Garcia-Orellana J (2017) Constraining the temporal variations of Ra isotopes and Rn in the groundwater end-member: implications for derived SGD estimates. Sci Total Environ 595:849–857

Chandler RV, Moorea JD, Gillett B (1985) Ground-water chemistry and salt-water encroachment, southern Baldwin County, Alabama. Geological Survey of Alabama Bulletin 126

Charette MA, Buesseler KO, Andrews JE (2001) Utility of radium isotopes for evaluating the input and transport of groundwater-derived nitrogen to a Cape Cod Estuary. Limnol Oceanogr 46:465–470

Charette MA, Splivallo R, Herbold C, Bollinger MS, Moore WS (2003) Salt marsh submarine groundwater discharge as traced by radium isotopes. Mar Chem 84:113–121

Cory RM, McKnight DM (2005) Fluorescence spectroscopy reveals ubiquitous presence of oxidized and reduced quinones in dissolved organic matter. Environ Sci Technol 39:8142–8149

Craig H (1957) Isotopic standards for carbon and oxygen and correction factors for mass-spectrometric analysis of carbon dioxide. Geochim Cosmochim Acta 12:133–149

D'Avanzo C, Kremer JN (1994) Diel oxygen dynamics and anoxic events in an eutrophic estuary of Waquoit Bay, Massachusetts. Estuaries 17:131–139

Diaz RJ, Rosenberg R (2008) Spreading dead zones and consequences for marine ecosystems. Science 32:926–929

Diepenbroek M, Glöckner FO, Grobe P, Güntsch A, Huber R, König-Ries B, Kostadinov I, Nieschulze J, Seeger B, Tolksdorf R, Triebel D. (2014) Towards an integrated biodiversity and ecological research data management and archiving platform: the German Federation for the Curation of Biological Data (GFBio). In: Informatik 2014

Ding L, Yokota A (2004) Proposals of *Curvibacter gracilis* gen. nov., sp. nov. and H*erbaspirillum putei* sp. nov. for bacterial strains isolated from well water and reclassification of [*Pseudomonas*] *huttiensis*, [*Pseudomonas*] *lanceolata*, [*Aquaspirillum*] *delicatum* and [*Aquaspirillum*] *autotrophicum* as *Herbaspirillum huttiense* comb. nov., *Curvibacter lanceolatus* comb. nov., *Curvibacter delicatus* comb. nov. and *Herbaspirillum autotrophicum* comb. nov. Int J Syst Evol Microbiol 54:2223–2230

Dinnel SP, Schroeder WW, Wiseman WJ Jr (1990) Estuarine-shelf exchange using Landsat images of discharge plumes. J Coast Res 6:789–799

Domangue RJ, Mortazavi B (2018) Nitrate reduction pathways in the presence of excess nitrogen in a shallow eutrophic estuary. Environ Pollut 238:599–606

Dowling CB, Poreda RJ, Hunt AG, Carey AE (2004) Ground water discharge and nitrate flux to the Gulf of Mexico. Groundwater 42:401–417

Du J, Park K, Shen J, Dzwonkowski B, Yu X, Yoon BI (2018) Role of baroclinic processes on flushing characteristics in a highly stratified estuarine system, Mobile Bay. Alabama. J Geophys Res Oceans. https://doi.org/10.1029/2018JC013855

Dulaiova H, Burnett W, Wattayakorn G, Sojisuporn P (2006) Are groundwater inputs into river-dominated areas important? The Chao Phraya River—Gulf of Thailand. Limnol Oceanogr 51:2232–2247

Dyer KR (1973) Estuaries: a physical introduction. Wiley, London

Dzwonkowski B, Fournier S, Reager JT, Milroy S, Park K, Shiller AM, Greer AT, Soto I, Dykstra SL, Sanial V (2018)

Tracking sea surface salinity and dissolved oxygen on a river-influenced, seasonally stratified shelf, Mississippi Bight, northern Gulf of Mexico. Cont Shelf Res 169:25–33

Ellis J (2013) Evaluation of submarine groundwater discharge and groundwater quality using a novel coupled approach: isotopic tracer techniques and numerical modeling. Master's Thesis, University of Alabama

Ellis JT, Spruce JP, Swann RA, Smoot JC, Hilbert KW (2011) An assessment of coastal land-use and land-cover change from 1974–2008 in the vicinity of Mobile Bay, Alabama. J Coast Conserv 15:139–149

Fellman JB, Spencer RGM, Hernes PJ, Edwards RT, D'Amore DV, Hood E (2010) The impact of glacier runoff on the biodegradability and biochemical composition of terrigenous dissolved organic matter in near-shore marine ecosystems. Mar Chem 121:112–122

Garcés E, Basterretxea G, Tovar-Sánchez A (2011) Changes in microbial communities in response to submarine groundwater input. Mar Ecol Prog Ser 438:47–58

Gardner WS, McCarthy MJ, An S, Sobolev D, Sell KS, Brock D (2006) Nitrogen fixation and dissimilatory nitrate reduction to ammonium (DNRA) support nitrogen dynamics in Texas estuaries. Limnol Oceanogr 51:558–568

Geological Survey of Alabama (2018) Assessment of groundwater resources in Alabama, 2010–16. Geological Survey of Alabama Bulletin 186

Gillett B, Raymond D, Moore J, Tew B (2000) Hydrogeology and vulnerability to contamination of major aquifers in Alabama: Area 13. Geological Survey of Alabama Circular 199A

Granger J, Sigman DM, Lehmann MF, Tortell PD (2008) Nitrogen and oxygen isotope fractionation during dissimilatory nitrate reduction by denitrifying bacteria. Limnol Oceanogr 53:2533–2545

Greene DL, Rodriguez AB, Anderson JB (2007) Seaward-branching coastal-plain and piedmont incised-valley systems through multiple sea-level cycles: Late Quaternary examples from Mobile Bay and Mississippi Sound, USA. J Sediment Res 77:139–158

Gruber N (2004) The dynamics of the marine nitrogen cycle and its influence on atmospheric CO_2 variations. In: Oguz T, Follows M (eds) Carbon climate interactions. Springer, Dordrecht, pp 97–148

Guerra R, Righi S, Garcia-Luque E (2015) Modern accumulation rates and sources of organic carbon in the NE Gulf of Cadiz (SW Iberian Peninsula). J Radioanal Nucl Chem 305:429–437

Hanson RS, Hanson TE (1996) Methanotrophic bacteria. Microbiol Rev 60:439–471

Harms NC, Lahajnar N, Gaye B, Rixen T, Dähnke K, Ankele M, Schwarz-Schampera U, Emeis KC (2019) Nutrient distribution and nitrogen and oxygen isotopic composition of nitrate in water masses of the subtropical southern Indian Ocean. Biogeosciences 16:2715–2732

Hattori S (2008) Syntrophic acetate-oxidizing microbes in methanogenic environments. Microbes Environ 23: 118–127

Hernes PJ, Bergamaschi BA, Eckard RS, Spencer RG (2009) Fluorescence-based proxies for lignin in freshwater dissolved organic matter. J Geophys Res Biogeosci. https://doi.org/10.1029/2009JG000938

Holmes AJ, Costello A, Lidstrom M, Murrell JC (1995) Evidence that participate methane monooxygenase and ammonia monooxygenase may be evolutionarily related. FEMS Microbiol Lett 132:203–208

Howarth R, Chan F, Conley DJ, Garnier J, Doney SC, Marino R, Billen G (2011) Coupled biogeochemical cycles: eutrophication and hypoxia in temperate estuaries and coastal marine ecosystems. Front Ecol Environ 9:18–26

Hummel RL (1996) Holocene Geologic History of the West Alabama Inner Continental Shelf, Alabama. Geological Survey of Alabama Bulletin 189

Hwang DW, Kim G, Lee YW, Yang HS (2005) Estimating submarine inputs of groundwater and nutrients to a coastal bay using radium isotopes. Mar Chem 96:61–71

Jarvis BDW, Van Berkum P, Chen WX, Nour SM, Fernandez MP, Cleyet-Marel JC, Gillis M (1997) Transfer of *Rhizobium loti*, *Rhizobium huakuii*, *Rhizobium ciceri*, *Rhizobium mediterraneum*, and *Rhizobium tianshanense* to *Mesorhizobium* gen. nov. Int J Syst Evol Microbiol 47:895–898

Johannes RE (1980) The ecological significance of the submarine discharge of groundwater. Mar Ecol Prog Ser 3:365–373

Kelly RP, Moran SB (2002) Seasonal changes in groundwater input to a well-mixed estuary estimated using radium isotopes and implications for coastal nutrient budgets. Limnol Oceanogr 47:1796–1807

Kendall C (1998) Tracing nitrogen sources and cycling in catchments. In: Kendall C, McDonnell JJ (eds) Isotope tracers in catchment hydrology. Elsevier, Amsterdam, pp 519–576

Kendall C, Elliott EM, Wankel SD (2007) Tracing anthropogenic inputs of nitrogen to ecosystems. In: Stable isotopes in ecology and environmental science, pp 375–449. https://doi.org/10.1002/9780470691854.ch12

Kim G, Swarzenski PW (2010) Submarine groundwater discharge (SGD) and associated nutrient fluxes to the coastal ocean. In: Liu K, Atkinson L, Quiñones R, Talaue-McManus L (eds) Carbon and nutrient fluxes in continental margins. Springer, Berlin, pp 529–538

Knee KL, Paytan A (2011) Submarine groundwater discharge: a source of nutrients, metals, and pollutants to the coastal ocean. In: Wolanski E, McLusky DS (eds) Treatise on estuarine and coastal science. Academic, Waltham, pp 205–233

Krantz DE, Manheim FT, Bratton JF, Phelan DJ (2004) Hydrogeologic setting and ground water flow beneath a section of Indian River Bay, Delaware. Groundwater 42:1035–1051

Krest JM, Moore WS, Gardner LR, Morris JT (2000) Marsh nutrient export supplied by groundwater discharge: evidence from radium measurements. Glob Biogeochem Cycles 14:167–176

Kroeger KD, Swarzenski PW, Greenwood WJ, Reich C (2007) Submarine groundwater discharge to Tampa Bay: nutrient fluxes and biogeochemistry of the coastal aquifer. Mar Chem 104:85–97

Kuever J (2014a) The Family Syntrophaceae. In: Rosenberg E, DeLong EF, Lory S, Stackebrandt E, Thompson F (eds) The prokaryotes. Springer, Berlin, pp 281–288

Kuever J (2014b) The Family Syntrophobacteraceae. In: Rosenberg E, DeLong EF, Lory S, Stackebrandt E, Thompson F (eds) The prokaryotes. Springer, Berlin, pp 289–299

Lamb AL, Wilson GP, Leng MJ (2006) A review of coastal palaeoclimate and relative sea-level reconstructions using $\delta^{13}C$ and C/N ratios in organic material. Earth Sci Rev 75:29–57

Lambert WJ, Aharon P, Rodriguez AB (2008) Catastrophic hurricane history revealed by organic geochemical proxies in coastal lake sediments: a case study of Lake Shelby, Alabama (USA). J Paleolimnol 39:117–131

Lee YW, Hwang DW, Kim G, Lee WC, Oh HT (2009) Nutrient inputs from submarine groundwater discharge (SGD) in Masan Bay, an embayment surrounded by heavily industrialized cities, Korea. Sci Total Environ 407:3181–3188

Liefer JD, MacIntyre HL, Novoveska L, Smith WL, Dorsey CP (2009) Temporal and spatial variability in *Pseudo-nitzschia* spp. in Alabama coastal waters: a hot spot linked to submarine groundwater discharge? Harmful Algae 8:706–714

Liefer JD, MacIntyre HL, Su N, Burnett WC (2014) Seasonal alternation between groundwater discharge and benthic coupling as nutrient sources in a shallow coastal lagoon. Estuaries Coasts 37:925–940

Liu X, Li M, Castelle CJ, Probst AJ, Zhou Z, Pan J, Liu Y, Banfield JF, Gu JD (2018) Insights into the ecology, evolution, and metabolism of the widespread Woesearchaeotal lineages. Microbiome 6:102

Loesch H (1960) Sporadic mass shoreward migrations of demersal fish and crustaceans in Mobile Bay, Alabama. Ecology 41:292–298

Lovley DR, Giovannoni SJ, White DC, Champine JE, Phillips EJP, Gorby YA, Goodwin S (1993) *Geobacter metallireducens* gen. nov. sp. nov., a microorganism capable of coupling the complete oxidation of organic compounds to the reduction of iron and other metals. Arch Microbiol 159:336–344

Lu YH, Edmonds JW, Yamashita Y, Zhou B, Jaegge A, Baxley M (2015) Spatial variation in the origin and reactivity of dissolved organic matter in Oregon–Washington coastal waters. Ocean Dyn 65:17–32

Macintyre HL, Stutes AL, Smith WL, Dorsey CP, Abraham A, Dickey RW (2011) Environmental correlates of community composition and toxicity during a bloom of *Pseudo-nitzschia* spp. in the northern Gulf of Mexico. J Plankton Res 33:273–295

Makings U, Santos IR, Maher DT, Golsby-Smith L, Eyre BD (2014) Importance of budgets for estimating the input of groundwater-derived nutrients to an eutrophic tidal river and estuary. Estuar Coast Shelf Sci 143:65–76

Mariotti A (1983) Atmospheric nitrogen is a reliable standard for natural ^{15}N abundance measurements. Nature 303:685

Maus I, Rumming M, Bergmann I, Heeg K, Pohl M, Nettmann E, Jaenicke S, Blom J, Pühler A, Schlüter A, Sczyrba A (2018) Characterization of Bathyarchaeota genomes assembled from metagenomes of biofilms residing in mesophilic and thermophilic biogas reactors. Biotechnol Biofuels 11:167

May EB (1973) Extensive oxygen depletion in Mobile Bay, Alabama. Limnol Oceanogr 18:353–366

McCoy C, Viso R, Peterson RN, Libes S, Lewis B, Ledoux J, Voulgaris G, Smith E, Sanger D (2011) Radon as an indicator of limited cross-shelf mixing of submarine groundwater discharge along an open ocean beach in the South Atlantic Bight during observed hypoxia. Cont Shelf Res 31:1306–1317

Meyers PA (1997) Organic geochemical proxies of paleoceanographic, paleolimnologic, and paleoclimatic processes. Org Geochem 27:213–250

Michael HA, Scott KC, Koneshloo M, Yu X, Khan MR, Li K (2016) Geologic influence on groundwater salinity drives large seawater circulation through the continental shelf. Geophys Res Lett. https://doi.org/10.1002/2016GL070863

Mitchell GJ, Jones JG, Cole JA (1986) Distribution and regulation of nitrate and nitrite reduction by *Desulfovibrio* and *Desulfotomaculum* species. Arch Microbiol 144:35–40

Mohamed NM, Saito K, Tal Y, Hill RT (2010) Diversity of aerobic and anaerobic ammonia-oxidizing bacteria in marine sponges. ISME J 4:38

Montiel D, Lamore A, Stewart J, Dimova N (2018) Is submarine groundwater discharge (SGD) important for the historical fish kills and harmful algal bloom events of Mobile Bay? Estuaries Coasts 42:470–493

Moore WS (1999) The subterranean estuary: a reaction zone of ground water and sea water. Mar Chem 65:111–125

Moore WS, Blanton JO, Joye SB (2006) Estimates of flushing times, submarine groundwater discharge, and nutrient fluxes to Okatee Estuary, South Carolina. J Geophys Res Oceans. https://doi.org/10.1029/2005JC003041

Moura I, Bursakov S, Costa C, Moura JJ (1997) Nitrate and nitrite utilization in sulfate-reducing bacteria. Anaerobe 3:279–290

Murgulet D, Tick GR (2009) Assessing the extent and sources of nitrate contamination in the aquifer system of southern Baldwin County, Alabama. Environ Geol 58:1051–1065

Murgulet D, Tick GR (2013) Understanding the sources and fate of nitrate in a highly developed aquifer system. J Contam Hydrol 155:69–81

Nercessian O, Noyes E, Kalyuzhnaya MG, Lidstrom ME, Chistoserdova L (2005) Bacterial populations active in metabolism of C1 compounds in the sediment of Lake Washington, a freshwater lake. Appl Environ Microbiol 71:6885–6899

Null KA, Corbett DR, DeMaster DJ, Burkholder JM, Thomas CJ, Reed RE (2011) Porewater advection of ammonium into the Neuse River Estuary, North Carolina, USA. Estuar Coast Shelf Sci 95:314–325

Null KA, Dimova NT, Knee KL, Esser BK, Swarzenski PW, Singleton MJ, Stacey M, Paytan A (2012) Submarine groundwater discharge-derived nutrient loads to San Francisco Bay: implications to future ecosystem changes. Estuaries Coasts 35:1299–1315

Nyerges G, Han SK, Stein LY (2010) Effects of ammonium and nitrite on growth and competitive fitness of cultivated methanotrophic bacteria. Appl Environ Microbiol 76: 5648–5651

Paerl HW (1997) Coastal eutrophication and harmful algal blooms: importance of atmospheric deposition and groundwater as "new" nitrogen and other nutrient sources. Limnol Oceanogr 42:1154–1165

Paerl HW, Pinckney JL, Fear JM, Peierls BL (1998) Ecosystem responses to internal and watershed organic matter loading: consequences for hypoxia in the eutrophying Neuse River Estuary, North Carolina, USA. Mar Ecol Prog Ser 166:17–25

Park K, Kim CK, Schroeder WW (2007) Temporal variability in summertime bottom hypoxia in shallow areas of Mobile Bay, Alabama. Estuaries Coasts 30:54–65

Peterson RN, Moore WS, Chappel SL, Viso RF, Libes SM, Peterson LE (2016) A new perspective on coastal hypoxia: the role of saline groundwater. Mar Chem 179:1–11

Prauser H (1976) *Nocardioides*, a new genus of the order Actinomycetales. Int J Syst Evol Microbiol 26:58–65

Rabalais NN, Turner RE, Wiseman WJ Jr (2002) Gulf of Mexico hypoxia, aka "The dead zone". Annu Rev Ecol Syst 33:235–263

Redfield AC (1934) On the proportions of organic derivatives in sea water and their relation to the composition of plankton. James Johnstone Memorial volume, pp 176–192

Reed PC (1971) Geologic map of Baldwin County, Alabama. Geological Survey of Alabama Special Map 94

Robertson WD (1995) Development of steady-state phosphate concentrations in septic system plumes. J Contam Hydrol 19:289–305

Rodellas V, García-Orellana J, Tovar-Sánchez A, Basterretxea G, López-García JM, Sánchez-Quiles D, García-Solsona E, Masqué P (2014) Submarine groundwater discharge as a source of nutrients and trace metals in a Mediterranean Bay (Palma Beach, Balearic Islands). Mar Chem 160:56–66

Rodriguez AB, Greene DL, Anderson JB, Simms AR (2008) Response of Mobile Bay and eastern Mississippi Sound, Alabama, to changes in sediment accommodation and accumulation. In: Anderson JB, Rodriguez AB (eds) Response of Upper Gulf Coast estuaries to Holocene climate change and sea-level rise. Geological Society of America, pp 13–29

Ryabenko E (2013) Stable isotope methods for the study of the nitrogen cycle. In: Zambianchi E (ed) Topics in oceanography. InTech, Rijeka, pp 1–40

Rysgaard S, Risgaard-Petersen N, Sloth NP (1996) Nitrification, denitrification, and nitrate ammonification in sediments of two coastal lagoons in southern France. In: Caumette P, Castel J, Herbert R (eds) Coastal lagoon eutrophication and anaerobic processes. Springer, Dordrecht, pp 133–141

Sadat-Noori M, Santos IR, Tait DR, Maher DT (2016) Fresh meteoric versus recirculated saline groundwater nutrient inputs into a subtropical estuary. Sci Total Environ 566:1440–1453

Sangwan P, Chen X, Hugenholtz P, Janssen PH (2004) *Chthoniobacter flavus* gen. nov., sp. nov., the first pure-culture representative of subdivision two, *Spartobacteria classis* nov., of the phylum Verrucomicrobia. Appl Environ Microbiol 70:5875–5881

Santos P, Pinhal I, Rainey FA, Empadinhas N, Costa J, Fields B, Benson R, Veríssimo A, da Costa MS (2003) Gamma-Proteobacteria *Aquicella lusitana* gen. nov., sp. nov., and *Aquicella siphonis* sp. nov. infect protozoa and require activated charcoal for growth in laboratory media. Appl Environ Microbiol 69:6533–6540

Santos IRS, Burnett WC, Chanton J, Mwashote B, Suryaputra IG, Dittmar T (2008) Nutrient biogeochemistry in a Gulf of Mexico subterranean estuary and groundwater-derived fluxes to the coastal ocean. Limnol Oceanogr 53:705–718

Santos IR, Burnett WC, Chanton J, Dimova N, Peterson RN (2009) Land or ocean? Assessing the driving forces of submarine groundwater discharge at a coastal site in the Gulf of Mexico. J Geophys Res Oceans 114:1–11

Schnurrenberger D, Russell J, Kelts K (2003) Classification of lacustrine sediments based on sedimentary components. J Paleolimnol 29:141–154

Schroeder WW, Wiseman WJ (1986) Low-frequency shelf-estuarine exchange processes in Mobile Bay and other estuarine systems on the northern Gulf of Mexico. In: Wolfe A (ed) Estuarine variability. Elsevier, Amsterdam, pp 355–367

Schroeder WW, Dinnel SP, Wiseman WJ (1990) Salinity stratification in a river-dominated estuary. Estuaries 13:145–154

Sebilo M, Billen G, Grably M, Mariotti A (2003) Isotopic composition of nitrate-nitrogen as a marker of riparian and benthic denitrification at the scale of the whole Seine River System. Biogeochemistry 63:35–51

Seitz HJ, Cypionka H (1986) Chemolithotrophic growth of *Desulfovibrio desulfuricans* with hydrogen coupled to ammonification of nitrate or nitrite. Arch Microbiol 146:63–67

Seitzinger SP, Kroeze C, Bouwman AF, Caraco N, Dentener F, Styles RV (2002) Global patterns of dissolved inorganic and particulate nitrogen inputs to coastal systems: recent conditions and future projections. Estuaries 25:640–655

Sekiguchi Y, Muramatsu M, Imachi H, Narihiro T, Ohashi A, Harada H, Hanada S, Kamagata Y (2008) *Thermodesulfovibrio aggregans* sp. nov. and *Thermodesulfovibrio thiophilus* sp. nov., anaerobic, thermophilic, sulfate-reducing bacteria isolated from thermophilic methanogenic sludge, and emended description of the genus *Thermodesulfovibrio*. Int J Syst Evol Microbiol 58:2541–2548

Shang P, Lu Y, Du Y, Jaffé R, Findlay RH, Wynn A (2018) Climatic and watershed controls of dissolved organic matter variation in streams across a gradient of agricultural land use. Sci Total Environ 612:1442–1453

Sigman DM, Casciotti KL, Andreani M, Barford C, Galanter M, Böhlke JK (2001) A bacterial method for the nitrogen isotopic analysis of nitrate in seawater and freshwater. Anal Chem 73:4145–4153

Slomp C, Van Cappellen P (2004) Nutrient inputs to the coastal ocean through submarine groundwater discharge: controls and potential impact. J Hydrol 295:64–86

Smith CG, Osterman LE (2014) An evaluation of temporal changes in sediment accumulation and impacts on carbon burial in Mobile Bay, Alabama, USA. Estuaries Coasts 37:1092–1106

Smith CG, Swarzenski PW (2012) An investigation of submarine groundwater-borne nutrient fluxes to the west Florida shelf and recurrent harmful algal blooms. Limnol Oceanogr 57:471–485

Spiteri C, Slomp CP, Charette MA, Tuncay K, Meile C (2008) Flow and nutrient dynamics in a subterranean estuary (Waquoit Bay, MA, USA): field data and reactive transport modeling. Geochim Cosmochim Acta 72:3398–3412

Stanek W, Silc T (1977) Comparisons of four methods for determination of degree of peat humification

(decomposition) with emphasis on the von Post method. Can J Soil Sci 57:109–117

Stanier R, Kunisawa R, Mandel M, Cohen-Bazire G (1971) Purification and properties of unicellular blue-green algae (order Chroococcales). Bacteriol Rev 35:171

Stedmon CA, Bro R (2008) Characterizing dissolved organic matter fluorescence with parallel factor analysis: a tutorial. Limnol Oceanogr Methods 6:572–579

Stumpf RP, Gelfenbaum G, Pennock JR (1993) Wind and tidal forcing of a buoyant plume, Mobile Bay, Alabama. Cont Shelf Res 13:1281–1301

Su N, Burnett WC, MacIntyre HL, Liefer JD, Peterson RN, Viso R (2014) Natural radon and radium isotopes for assessing groundwater discharge into Little Lagoon, AL: implications for harmful algal blooms. Estuaries Coasts 37: 893–910

Sun L, Toyonaga M, Ohashi A, Tourlousse DM, Matsuura N, Meng XY, Tamaki H, Hanada S, Cruz R, Yamaguchi T, Sekiguchi Y (2016) *Lentimicrobium saccharophilum* gen. nov., sp. nov., a strictly anaerobic bacterium representing a new family in the phylum Bacteroidetes, and proposal of Lentimicrobiaceae fam. nov. Int J Syst Evol Microbiol 66:2635–2642

Tiedje JM (1988) Ecology of denitrification and dissimilatory nitrate reduction to ammonium. Biol Anaerob Microorg 717:179–244

Turner R, Schroeder W, Wiseman WJ (1987) The role of stratification in the deoxygenation of Mobile Bay and adjacent shelf bottom waters. Estuaries 10:13–19

Valiela I, Costa J, Foreman K, Teal JM, Howes B, Aubrey D (1990) Transport of groundwater-borne nutrients from watersheds and their effects on coastal waters. Biogeochemistry 10:177–197

Valiela I, Geist M, McClelland J, Tomasky G (2000) Nitrogen loading from watersheds to estuaries: verification of the Waquoit Bay nitrogen loading model. Biogeochemistry 49:277–293

Walter GR, Kidd RE (1979) Ground-water management techniques for the control of salt-water encroachment in Gulf Coast aquifers, a summary report. Geological Survey of Alabama Open-file Report, p 84

Ward GM, Harris PM, Ward AK (2005) Gulf Coast rivers of the southeastern United States. In: Benke AC, Cushing CE (eds) Rivers of North America. Elsevier Press, Burlington, pp 125–178

Watson SW, Bock E, Valois FW, Waterbury JB, Schlosser U (1986) *Nitrospira marina* gen. nov. sp. nov.: a chemolithotrophic nitrite-oxidizing bacterium. Arch Microbiol 144:1–7

Weiskel PK, Howes BL (1992) Differential transport of sewage-derived nitrogen and phosphorus through a coastal watershed. Environ Sci Technol 26:352–360

Weiss JV, Rentz JA, Plaia T, Neubauer SC, Merrill-Floyd M, Lilburn T, Bradburne C, Megonigal JP, Emerson D (2007) Characterization of neutrophilic Fe(II)-oxidizing bacteria isolated from the rhizosphere of wetland plants and description of *Ferritrophicum radicicola* gen. nov. sp. nov., and *Sideroxydans paludicola* sp. nov. Geomicrobiol J 24:559–570

Wheeler KI, Levia DF, Hudson JE (2017) Tracking senescence-induced patterns in leaf litter leachate using parallel factor analysis (PARAFAC) modeling and self-organizing maps. J Geophys Res Biogeosci 122:2233–2250

Widdel F, Pfennig N (1982) Studies on dissimilatory sulfate-reducing bacteria that decompose fatty acids II. Incomplete oxidation of propionate by *Desulfobulbus propionicus* gen. nov., sp. nov. Arch Microbiol 131:360–365

Wolfe DA, Kjerfve B (1986) Estuarine variability: an overview. In: Wolfe DA (ed) Estuarine variability. Elsevier, Amsterdam, pp 3–17

Xu B, Burnett W, Dimova N, Diao S, Mi T, Jiang X, Yu Z (2013) Hydrodynamics in the Yellow River Estuary via radium isotopes: ecological perspectives. Cont Shelf Res 66:19–28

Xue D, Botte J, De Baets B, Accoe F, Nestler A, Taylor P, Van Cleemput O, Berglund M, Boeckx P (2009) Present limitations and future prospects of stable isotope methods for nitrate source identification in surface- and groundwater. Water Res 43:1159–1170

Yamada T, Sekiguchi Y, Hanada S, Imachi H, Ohashi A, Harada H, Kamagata Y (2006) *Anaerolinea thermolimosa* sp. nov., *Levilinea saccharolytica* gen. nov., sp. nov. and *Leptolinea tardivitalis* gen. nov., sp. nov., novel filamentous anaerobes, and description of the new classes *Anaerolineae classis* nov. and *Caldilineae classis* nov. in the bacterial phylum Chloroflexi. Int J Syst Evol Microbiol 56: 1331–1340

Yamaguchi M, Itakura S, Uchida T (2001) Nutrition and growth kinetics in nitrogen- or phosphorus-limited cultures of the 'novel red tide' dinoflagellate *Heterocapsa circularisquama* (Dinophyceae). Phycologia 40:313–318

Yamashita Y, Jaffé R, Maie N, Tanoue E (2008) Assessing the dynamics of dissolved organic matter (DOM) in coastal environments by excitation emission matrix fluorescence and parallel factor analysis (EEM-PARAFAC). Limnol Oceanogr 53:1900–1908

Yevenes M, Soetaert K, Mannaerts C (2016) Tracing nitrate-nitrogen sources and modifications in a stream impacted by various land uses, south Portugal. Water 8:385

Zanini L, Robertson WD, Ptacek CJ, Schiff SL, Mayer T (1998) Phosphorus characterization in sediments impacted by septic effluent at four sites in central Canada. J Contam Hydrol 33:405–429